(2) LEVEL II

NRL Memorandum Report 4663

AD A111 027

The Three-Dimensional Non-Linear Theory of the Free Electron Laser in the Amplifying Configuration

P. SPRANGLE AND CHA-MEI TANG

Plasma Physics Division

December 28, 1981

NAVAL RESEARCH LABORATORY
Washington, D.C.

Approved for public release; distribution unlimited.

REPORT DOCUMENTATION PAGE

READ INSTRUCTIONS BEFORE COMPLETING FORM

1. REPORT NUMBER NRL Memorandum Report 4663	2. GOVT ACCESSION NO. AD-A110 227	3. RECIPIENT'S CATALOG NUMBER
4. TITLE (and Subtitle) THE THREE-DIMENSIONAL NON-LINEAR THEORY OF THE FREE ELECTRON LASER IN THE AMPLIFYING CONFIGURATION		5. TYPE OF REPORT & PERIOD COVERED Interim report on a continuing NRL problem 6. PERFORMING ORG. REPORT NUMBER
7. AUTHOR(s) P. Sprangle and Cha-Mei Tang		8. CONTRACT OR GRANT NUMBER(s)
9. PERFORMING ORGANIZATION NAME AND ADDRESS Naval Research Laboratory Washington, D.C. 20375		10. PROGRAM ELEMENT, PROJECT, TASK AREA & WORK UNIT NUMBERS 47-0867-0-1 ARPA Order No. 3817 P.E. 62301E
11. CONTROLLING OFFICE NAME AND ADDRESS Defense Advanced Research Projects Agency Arlington, VA 22209		12. REPORT DATE December 28, 1981 13. NUMBER OF PAGES 44
14. MONITORING AGENCY NAME & ADDRESS(if different from Controlling Office)		15. SECURITY CLASS. (of this report) UNCLASSIFIED 15a. DECLASSIFICATION/DOWNGRADING SCHEDULE

16. DISTRIBUTION STATEMENT (of this Report)

Approved for public release; distribution unlimited.

17. DISTRIBUTION STATEMENT (of the abstract entered in Block 20, if different from Report)

18. SUPPLEMENTARY NOTES

19. KEY WORDS (Continue on reverse side if necessary and identify by block number)

Free electron laser
Amplifier

20. ABSTRACT (Continue on reverse side if necessary and identify by block number)

This paper presents a self-consistent non-linear treatment of the finite transverse dimensional effects associated with (i) the wiggler field, (ii) the electron beam and (iii) the radiation beam of the free electron laser (FEL) in a steady state amplifying configuration. Our formulation incorporates various efficiency enhancement schemes. A linearly polarized magnetic wiggler is used for our formulation. The inherent gradient of the magnetic wigglers in the transverse direction introduces betatron oscillations, which cause an increase in the effective axial beam temperature.

(Continued)

DD FORM 1473 1 JAN 73 EDITION OF 1 NOV 65 IS OBSOLETE
S/N 0102-014-6601

20. ABSTRACT (Continued)

The radiation beam in the presence of the electron beam and the magnetic wiggler experience diffraction as well as refraction effects. We find that the 3-D effects can lead to substantial differences in the results compared to the 1-D theory. Finally a 3-D numerical illustration of a 10.6 μm FEL is given.

CONTENTS

THE THREE-DIMENSIONAL NON-LINEAR THEORY OF THE FREE ELECTRON LASER IN THE AMPLIFYING CONFIGURATION

I. INTRODUCTION

The development of lasers in which the active medium is a relativistic beam of electrons has recently evoked much interest. These radiation sources can be characterized by frequency tunability with output wavelength ranging from millimeter to beyond the optical regime, very high power levels, and high efficiencies.

The purpose of this paper is to present a non-linear 3-D formulation of the FEL in the steady state amplifying configuration including the various efficiency improvement schemes. The 3-D effects are associated with the wiggler field, the electron beam and the radiation beam. We find that the 3-D effects can lead to significantly different results than results obtained from the 1-D theory. Numerous publications have treated the 1-D free electron laser mechanism[1-14], while 3-D effects in the FEL have just recently been considered.[15-20]

The transverse effects associated with a static magnetic wiggler field introduces modifications in the electron dynamics. A physically realizable magnetic wiggler field has transverse spatial variations as well as an axial component of the magnetic field in order to satisfy $\nabla \times \mathbf{B}_w = \nabla \cdot \mathbf{B}_w = 0$. The physically realizable wiggler fields causes slow betatron oscillations, which result in an increase in the effective axial beam temperature. If the effective beam temperature is large, it will significantly reduce the fraction of electrons trapped in the ponderomotive potential buckets.

The effects of finite transverse dimensions of the radiation and electron beam are interrelated. The radiation beam can be considered to be a superposition of the input field and excited field. The input Gaussian radiation beam diffracts as it propagates through the interaction region; its amplitude and phase change as a function of axial position. The excited radiation beam suffers from both diffraction and refraction. The profile of the excited radiation beam is in general not Gaussian. The waist of the input field is typically somewhat greater than the electron beam radius, whereas the effective waist of the excited field is comparable to the radius of the electron beam and hence it diffracts more rapidly than the input field. In general, the potential exists for destructive interference between the two fields. This would result in a decrease in the depth of the ponderomotive potential wells and cause detrapping of the electrons. However, destructive interference, in the parameter regime which we consider, is not observed.

Manuscript submitted October 28, 1981.

A number of efficiency enhancement schemes[7,10,11] for the FEL have been identified. Improved efficiency can be achieved by any or all of the following methods: (i) contouring, spatially in the longitudinal direction, the amplitude and/or wavelength of the magnetic wiggler field, and (ii) applying an external D.C. electric field. By applying one or more of these efficiency enhancement schemes, the phase of the electrons trapped in the ponderomotive wave can be adjusted so that electron kinetic energy is converted into radiation. Our formulation will include and show the equivalence of the above enhancement schemes.

In Section II, we describe the 3-D particle dynamics in a linearly polarized magnetic wiggler. We obtain a general 3-D solution for the radiation field using Fourier transform techniques in Section III. Section IV is devoted to a FEL operating in the low gain limit with an electron beam possessing an axially symmetric Gaussian beam profile. Section V derives the expression for total power gain and efficiency. In the last section, we give a numerical example of an FEL operating at 10.6 μm.

II. PARTICLE DYNAMICS—DERIVATION OF PHASE EQUATION

Our model of the FEL configuration is shown in Figure 1. We consider a linearly polarized magnetic wiggler field that is independent of x. The generalized linearly polarized wiggler and radiation field are represented by the following vector potentials.

$$\mathbf{A}_w(y,z) = A_w(z)\cosh\left(k_w(z)y\right)\cos\left(\int_0^z k_w(z')dz'\right)\hat{e}_x, \tag{1}$$

$$\mathbf{A}_R(x,y,z,t) = A_R(x,y,z)\sin\left(\frac{\omega}{c}z - \omega t + \varphi(x,y,z)\right)\hat{e}_x, \tag{2}$$

where $A_w(z)$ and $k_w(z) = 2\pi/l_w(z)$ are the slowly varying amplitude and wave number of the wiggler field, l_w is the wiggler wavelength, A_R and φ are the slowly varying amplitude and phase of the total radiation field, ω is the frequency of the radiation and c is the speed of light.

We also include an external D.C. electric field $\mathbf{E}_{DC}(z) = -\partial\phi_{DC}(z)/\partial z\,\hat{e}_z$. In all cases of interest $|\mathbf{A}_w| >> |\mathbf{A}_R|$ by many orders of magnitude. Furthermore, it is necessary to have $k_w r_b << 1$ where r_b is the electron beam radius.[4]

Space charge effects will be neglected. This is appropriate if the beam density satisfies[16]

$$n_0 << (k_w^2\gamma_{z0}^4 A_w A_R)(2\pi\gamma_0 m_0 c^2)^{-1} \tag{3}$$

where $\gamma_{z0} = (1 - v_{z0}^2/c^2)^{-1/2}$, v_{z0} is the axial velocity of the electron in the wiggler field, $\gamma_0 = (1 - v_0^2/c^2)^{-1/2}$, and v_0 is the magnitude of the total particle velocity. Equation (3) can be derived by comparing the ponderomotive term to the space charge term in the pendulum equation or the equation for phase, see Ref. (8).

Electrons execute complicated trajectories in three-dimensions. If the radiation field, $A_R(x,y,z)$, varies little in the x-direction over the electron beam, there is a constant of motion in the x-direction

$$\mathbf{P}_x = \frac{|e|}{c} (\mathbf{A}_w + \mathbf{A}_R) \cdot \hat{e}_x. \tag{4}$$

The particles execute betatron types of orbits in the y-direction due to the gradient in the magnetic wiggler field. If a particle entered the interaction region $z = 0$ with transverse coordinates (x_0, y_0), and initial transverse velocity v_{y0}, the particle's transverse location at z is

$$\tilde{x} = x_0 + \frac{\beta_{\perp}}{k_w} \cosh\, (k_w(z)\tilde{y}) \sin \int_0^z k_w(z')\, dz' \tag{5a}$$

and

$$\tilde{y} = y_0 \cos K_0 z + \frac{v_{y_0}}{K_0 v_{z0}} \sin K_0 z \tag{5b}$$

where $\beta_{\perp} = v_{\perp}/c$, $v_{\perp} = |e| A_w/(\gamma_0 m_0 c)$ is the wiggle velocity, $\gamma_0 = (1 - v_0^2/c^2)^{-1/2}$, v_0 is the magnitude of total particle velocity and $K_0 = \beta_{\perp}\, k_w/\sqrt{2}$. The derivation of the betatron oscillation is given in Appendix I.

The envelope of the electron beam in the y direction is not a constant in general. For example, if there is no initial transverse velocity spread in the y direction, i.e., $v_{y0} = 0$, the electron beam undergoes periodic pinching in the y-direction. All realizable electron beams have finite emittance. The emittance, ϵ_y, is defined as $\epsilon_y = \pi y_{0,\max} (v_{y_{0,\max}}/c)$, where $y_{0,\max}$ and $v_{y_{0,\max}}$ are the electron beam waist and the maximum velocity spread respectively in the y-direction at the entrance of the magnetic wiggler. The condition for the envelope of the electron beam to remain approximately constant inside the realizable wiggler with transverse gradient is to require that the first and second term on the right-hand-side of (5b) be equal, i.e.,

$$y_{0,\max} = v_{y_{0,\max}}/(K_0 v_{z0}) = \sqrt{\epsilon_y/(\pi K_0)}. \tag{6a}$$

The condition[15(i)] on $y_{0,\max}$ in (6a) also leads to the smallest electron beam radius inside the wiggler field,

$$r_b = \sqrt{\frac{2\epsilon_y}{\pi K_0}}. \tag{6b}$$

The gradient in the wiggler field will lead to an increase in the energy spread associated with the axial motion. Let us consider a cold electron beam with total energy $\gamma_0 m_0 c^2$. Since part of the energy is associated with the transverse motion, the axial velocity of a particle decreases as the amplitude of the betatron oscillation increases. The maximum axial velocity shear, due to the wiggler gradient, is given by

$$\Delta v_{shear} = c(\beta_{0\perp} k_w r_b/2)^2, \tag{7}$$

while the corresponding longitudinal energy spread is

$$\Delta E_{shear} = \gamma_{0z}^2 \gamma_0 (\Delta v_{shear}/c) m_0 c^2. \tag{8}$$

One efficiency enhancement approach is to initially trap a large fraction of the electrons in the ponderomotive potential wells and adiabatically extract kinetic energy from the particles. In order to trap a substantial fraction of the electrons, we require the trapping potential to be larger or at least comparable to the axial particle energy spread, i.e., $|e|\phi_{trap} > \Delta E_{shear}$. The initial depth of the trapping potential is

$$|e|\phi_{trap}/(\gamma_0 m_0 c^2) = 2\sqrt{2}\gamma_{0z}\beta_{0\perp} (A_R/A_w)^{1/2}. \tag{9}$$

Combining Eqs. (7), (8) and (9), the radius of the electron beam is found to be limited by

$$r_b < (\gamma_{0z} k_w)^{-1} \left(\frac{8\sqrt{2}\gamma_{0z}}{\beta_{0\perp}}\right)^{1/2} \left(\frac{A_R}{A_w}\right)^{1/4}. \tag{10}$$

The axial electron dynamics is most crucial in the FEL mechanism. With this in mind, we start with the equation of motion for the axial electron velocity, which can be written in the form

$$\frac{dv_z}{dt} = \frac{|e|}{\gamma_z^2 \gamma m_0} \frac{\partial \phi_{DC}}{\partial z} - \frac{|e|^2}{2\gamma^2 m_0^2 c^2} \left[\frac{\partial}{\partial z}\left(A_w \cosh(k_w y) \cos\left(\int_0^z k_w dz'\right)\right)^2 \right.$$

$$\left. + 2k_w A_w \cosh(k_w y) A_R \cos\left(\int_0^z \left(\frac{\omega}{c} + k_w\right) dz' - \omega t + \varphi\right)\right] \tag{11}$$

where $v_z = v_z(x,y,z,t)$ is the axial electron velocity, $\gamma_z = (1 - v_z^2/c^2)^{-1/2}$, $\gamma = \gamma_z \gamma_{\perp}$, $\gamma_{\perp}(z) = (1 + (|e|\mathbf{A}_w(z)/(m_0 c^2))^2)^{1/2}$. In obtaining Eq. (11) we have taken $\omega \approx \gamma_z^2(1 + v_z/c)\, ck_w$ and the x component of electron momentum to be $(|e|/c)\, (\mathbf{A}_w(y,z) + \mathbf{A}_R(x,y,z,t)) \cdot \hat{e}_x$.

The second term on the right-hand side of Eq. (11) indicates that the axial velocity in a linearly polarized wiggler has an oscillatory component at twice the wiggler wave number. In Ref. (14), we showed that the axial oscillation is not large enough to cause particle detrapping in the ponderomotive potential well and, thus, it does not have a qualitative effect on the FEL mechanism.

At this point we perform a transformation[7] from the Eulerian independent variables x,y,z,t, to Lagrangian independent variables z, ψ_0, x_0, y_0, v_{y0} where ψ_0, x_0, y_0, v_{y0} are the particle's phase in the ponderomotive potential wave, transverse coordinates and transverse velocity at the entrance to the interaction region, i.e., $z = 0$.

The equation governing the relative phase between the electrons and the ponderomotive wave (see Ref. (8) for 1-D derivation) is given by the generalized pendulum like equation

$$\frac{\partial^2 \tilde{\psi}}{\partial z^2} = \frac{d^2 \varphi}{dz^2} + \frac{dk_w}{dz} + \frac{|e|\omega/c}{\tilde{\gamma}_z^2 \tilde{\gamma} m_0 c^2} \frac{\partial \phi_{DC}}{\partial z}$$

$$- \frac{|e|^2 \omega/c}{2\tilde{\gamma}^2 m_0^2 c^4} \left[\frac{\partial}{\partial z} \left\{ A_w \cosh(k_w \tilde{y}) \cos \int_0^z k_w dz' \right\}^2 \right. \tag{12}$$

$$\left. + 2 k_w A_w \cosh(k_w \tilde{y}) \; A_R(\tilde{x}, \tilde{y}, z) \cos \tilde{\psi} \right]$$

where $\tilde{\psi}(z, \psi_0, x_0, y_0, v_{y0}) = \int_0^z (\omega/c + k_w(z') - \omega/v_z(\tilde{x}, \tilde{y}, \psi_0, z'))\, dz' + \varphi(\tilde{x}, \tilde{y}, z) + \psi_0$ is the phase, $\tilde{\gamma} = \tilde{\gamma}_z \gamma_\perp$, $\tilde{\gamma}_z = (1 - \tilde{v}_z^2/c^2)^{-1/2}$, $\tilde{v}_z = \omega/(\omega/c + k_w(z) - \partial\tilde{\psi}/\partial z + d\varphi/dz)$ is the electron axial velocity and ψ_0 is the initial phase at $z = 0$.

Equations (5) and (12) completely describe the non-linear particle dynamics in terms of the fields $\mathbf{A}_w$ and $\mathbf{A}_R$. From the structure of Eq. (12), it becomes clear that contouring the wiggler wavelength and/or amplitude, i.e., dk_w/dz or dA_w^2/dz, is directly equivalent to applying D.C. electric field, i.e., $\partial\phi_{DC}/\partial z$.

III. EVOLUTION OF GENERAL 3-D TOTAL RADIATION FIELD

This section will derive the total radiation field in the presence of the electron beam. The radiation field satisfies the wave equation

$$\left(\nabla^2 - \frac{1}{c^2} \frac{\partial^2}{\partial t^2} \right) \mathbf{A}_R = - \frac{4\pi}{c} J_x \hat{e}_x \tag{13}$$

where the current density[7] is given by

$$J_x(x, y, z, t) = - \frac{|e| n_0 v_0}{\omega} \int_{-\infty}^{\infty} d\psi_0 \int_{-\infty}^{\infty} dx_0 \int_{-\infty}^{\infty} dy_0 \int_{-\infty}^{\infty} dv_{y0} \tag{14}$$

$$\sigma(v_{y0})\, \theta(x_0, y_0)\, \delta(x - \tilde{x})\, \delta(y - \tilde{y})\, \delta(t - \tilde{t}) \frac{\tilde{P}_x}{\tilde{P}_z}$$

where $\theta(x_0, y_0)$ is a function which describes the initial electron beam profile, $\sigma(v_{y0})$ is a function which describes the initial transverse velocity profile in y direction, n_0 is the electron beam density on axis outside of the interaction region, $\tilde{P}_x \simeq (|e|/c)\, \mathbf{A}_w(\tilde{y}, z) \cdot \hat{e}_x$ is the equilibrium particle momentum in the x-direction, and $\tilde{P}_z = \tilde{\gamma} m_0 \tilde{v}_z$ is the axial particle momentum. We can solve for $\mathbf{A}_R$ using Fourier transform techniques.

The radiation field in (2) can be represented in the form

$$\mathbf{A}_R(x,y,z,t) = (2i)^{-1} a(x,y,z) \exp i(\omega z/c - \omega t)\hat{e}_x + c.c. \tag{15}$$

where $a = A_R \exp(i\varphi)$ is the complex field amplitude. A_R and φ are slowly varying functions of z. Substituting (15) into the wave Eq. (13), we obtain an equation for $a(x,y,z)$,

$$\left[\frac{\partial^2}{\partial x^2} + \frac{\partial^2}{\partial y^2} + 2i\frac{\omega}{c}\frac{\partial}{\partial z}\right] a(x,y,z) = j(x,y,z), \tag{16}$$

where

$$j(x,y,z) = -\frac{4\omega i}{c}\int_0^{2\pi/\omega} dt\, J_x(x,y,z,t)\, e^{-i(\frac{\omega}{c}z - \omega t)}.$$

By applying arguments presented in Ref. (7), the integral over time can be eliminated. The variable $j(x,y,z)$ can now be rewritten as

$$j(x,y,z) = \frac{\omega_b^2}{c^2}\, i \int_0^{2\pi}\frac{d\psi_0}{2\pi}\int_{-\infty}^{\infty} dx_0 \int_{-\infty}^{\infty} dy_0\, \theta(x_0,y_0)\int_{-\infty}^{\infty} d\mathrm{v}_{y0} \tag{17}$$

$$\sigma(\mathrm{v}_{y0})\,\delta(x-\tilde{x})\delta(y-\tilde{y})\,\frac{A_w}{\tilde{\gamma}}\cosh(k_w\tilde{y})\exp(-i(\tilde{\psi}-\varphi)).$$

where $\omega_0 = (4\pi|e|^2 n_0/m_0)^{1/2}$ is the plasma frequency, $\tilde{x},\tilde{y}$ and $\tilde{\psi}$ are functions of $(z,\psi_0,x_0,y_0,\mathrm{v}_{y0})$. The term that is not resonant with the ponderomotive wave is dropped from $j(x,y,z)$.

The solution for $a(x,y,z)$ can be easily obtained by going to the transformed space. Let $\bar{f}$ be the Fourier transform of f,

$$\bar{f}(k_x,k_y,z) = \int_{-\infty}^{\infty} dx \int_{-\infty}^{\infty} dy\, f(x,y,z)\, e^{-i(k_x x + k_y y)}. \tag{18}$$

Equation (16) becomes

$$\left[-(k_x^2+k_y^2) + 2i\frac{\omega}{c}\frac{\partial}{\partial z}\right]\bar{a}(k_x,k_y,z) = \bar{j}(k_x,k_y,z). \tag{19}$$

Equation (19) can be easily integrated in z to yield $\bar{a}$ in terms of $\bar{j}$. The complex field amplitude $a(x,y,z)$ can be obtained by taking the inverse transform.

$$a(x,y,z) = \frac{1}{(2\pi)^2}\int_{-\infty}^{\infty}\int_{-\infty}^{\infty}\bar{a}(k_x,k_y,0)\, e^{i(k_x x + k_y y - \frac{k^2 z}{2\omega/c})}\, dk_x\, dk_y$$

$$-\frac{i}{2\omega/c}\frac{1}{(2\pi)^2}\int_0^z\int_{-\infty}^{\infty}\int_{-\infty}^{\infty}\bar{j}(k_x,k_y,z')\, e^{i(k_x x + k_y y - \frac{k^2(z-z')}{2\omega/c})}\, dk_x\, dk_y\, dz', \tag{20}$$

where $k^2 = k_x^2 + k_y^2$. We can write $a = a_{in} + a_{ex}$, where a_{in} is the input radiation field (homogeneous solution) represented by the first term on the right-hand-side of (20), and a_{ex} is the excited radiation field (particular solution) represented by the second term.

Since the homogeneous solution is the input radiation field, the only field at $z = 0$ is a_{in} and

$$\bar{a}(k_x,k_y,0) = \int_{-\infty}^{\infty}\int_{-\infty}^{\infty} a(x,y,0)\exp(-i(k_x x + k_y y))\, dxdy.$$

Taking the input field to be the lowest order Gaussian radiation beam we find

$$a_{in}(x,y,z) = A_{in}\frac{1}{\sqrt{1+(z/z_0)^2}}\exp\left[\frac{-z_0^2 r^2/r_0^2}{(z^2+z_0^2)}\right] \exp\left\{i\left(\frac{z_0 z}{z^2+z_0^2}\left(\frac{r^2}{r_0^2}\right) - \tan^{-1}\left(\frac{z}{z_0}\right)\right)\right\} \tag{21}$$

where A_{in} is the amplitude of the input field, r_0 is the minimum waist, $z_0 = r_0^2\,\omega/2c$ is the Rayleigh length of the input field.

The excited field in Eq. (20) can be rewritten in the form of convolution integrals,

$$a_{ex}(x,y,z) = \frac{-i}{2\omega/c}\int_0^z dz'\int_{-\infty}^{\infty} dx'\int_{-\infty}^{\infty} dy'\; G(x-x', y-y', z-z')\, j\,(x',y',z') \tag{22}$$

where

$$G(x,y,z) = \frac{1}{(2\pi)^2}\int_{-\infty}^{\infty} dk_x\int_{-\infty}^{\infty} dk_y\, \exp[-i\frac{(k_x^2+k_y^2)z}{2\omega/c}]\exp[i(k_x x+k_y y)]$$

$$= -i\frac{\omega/c}{2\pi}\,\frac{1}{z}\,\exp\left[i\left(\frac{x^2+y^2}{2z}\right)\frac{\omega}{c}\right] \tag{23}$$

is the Green's function. Substituting the expression for the current (17) into (22), the excited radiation field is found to be

$$a_{ex}(x,y,z) = -\frac{i}{4\pi}\frac{\omega_b^2}{c^2}\int_0^z dz'\int_0^{2\pi}\frac{d\psi_0}{2\pi}\int_{-\infty}^{\infty} dx_0\int_{-\infty}^{\infty} dy_0\int_{-\infty}^{\infty} dv_{y0}\; \sigma(v_{y0})\,\theta(x_0,y_0)\,\frac{A_w'}{\bar{\gamma}'}\cosh\,(k_w'\bar{y}')\frac{1}{z-z'} \exp\left[i((x-\bar{x}')^2+(y-\bar{y}')^2)\frac{\omega/c}{2(z-z')}\right]\exp\,[-i(\bar{\psi}'-\varphi')] \tag{24}$$

where the primes on quantities denote functions of z'. Equations (5), (12) and (24) describe self-consistently a general nonlinear 3-D steady state FEL amplifier.

IV. ANALYTIC AXIALLY SYMMETRIC SOLUTION

For purposes of illustrating transverse effects in the radiation field, we will consider a FEL having axial symmetry and operating in the low gain limit, i.e., $|a_{in}| >> |a_{ex}|$. We chose a Gaussian electron beam profile, $\theta = \exp(-(x_0^2 + y_0^2)/r_b^2)$, where r_b is the radius of the electron beam. If r_b satisfies Eqs. (6) and (10) and $k_w r_b << 1$, then we can neglect the gradient in the wiggler and replace $\tilde{x}$, $\tilde{y}$ in Eq. (24) by x_0, y_0 and $\sigma(v_{y0})$ by $\delta(v_{y0})$. For a low gain FEL and a plane wave input field, a_{in}, (or Gaussian like TEM_{00} radiation field with the waist of the radiation beam r_0 much larger than the radius of the electron beam) the phase $\tilde{\psi}$ is very nearly a function of z and ψ_0 only. With these simplifying assumptions, equation (24) can be integrated to give

$$a_{ex}(r,z) = -\frac{i}{4}\,\frac{\omega_b^2/c^2}{\gamma_0}\,r_b^2 \int_0^{2\pi} \frac{d\psi_0}{2\pi} \int_0^z dz'\, A_w(z')\, e^{i\varphi(z')} \tag{25}$$

$$\left(\frac{z - z' + iz_b}{(z - z')^2 + z_b^2}\right) \exp -i\left(\tilde{\psi}(z',\psi_0) - z_b\left(\frac{z - z' + iz_b}{(z - z')^2 + z_b^2}\right)\frac{r^2}{r_b^2}\right)$$

where $z_b = r_b^2\,\omega/2c$ is the effective Rayleigh length associated with the excited radiation. The excited radiation can be written in a more familiar form,

$$\mathbf{A}_{ex}(r,z,t) = \frac{\omega_b^2 r_b^2}{4c^2\gamma_0} \int_0^{2\pi} \frac{d\psi_0}{2\pi} \int_0^z dz' A_w(z')\, \frac{e^{\frac{-z_b^2 r^2/r_b^2}{(z - z')^2 + z_b^2}}}{\sqrt{(z - z')^2 + z_b^2}} \tag{26}$$

$$\cos\left(\frac{\omega}{c} z - \omega t - \tan^{-1}\left(\frac{z - z'}{z_b}\right) + \frac{z_b(z - z')}{(z - z')^2 + z_b^2}\left(\frac{r^2}{r_b^2}\right)\right.$$

$$\left. - \tilde{\psi}(z',\psi_0) + \varphi(z')\right)\hat{e}_x.$$

The excited radiation has a very simple interpretation. Each cross section of the electron beam produces an Gaussian like TEM_{00} radiation beam (see Eq. (21)) propagating to the right with the minimum spot size equal to the electron beam radius. The total excited radiation at a location $z = L$ down stream is the sum of all the Gaussian radiation beams which originated from $z = 0$ to L, see Fig. 2.

A square or Lorentzian electron beam profile may also be readily integrated in (24). The 1-D limit of (26) is obtained by letting z_b or r_b approach infinity.

We will now make the constant phase, resonant particle approximation. In this approximation all particles are assumed to have the same constant phase, $\tilde{\psi}_R$. The electron beam in this approximation consists of a pulse train of macro particles separated in distance by $2\pi v_{0z}/\omega$. Furthermore, we will limit ourselves at this point to a constant parameter wiggler and consider only an external D.C. electric potential. The rate of change, on axis, of the resonant particle energy is

$$\frac{\partial(\gamma_R m_0 c^2)}{\partial z} = |e| \frac{\partial \phi_{DC}(z)}{\partial z} - \frac{|e|^2 \omega/c}{2\gamma_R m_0 c^2} A_w A_R(r = 0, z) \cos \tilde{\psi}_R. \tag{27}$$

To obtain the total radiation field, we first evaluate $a_{ex}(r,z)$ under the assumption that $|\varphi| << 1$ (this will be shown later to be valid). The excited resonant particle radiation a_{ex} for all r and z is

$$a_{ex}(r,z) = -i\,\alpha_0^2 A_w \left[E_i\left(\frac{-r^2}{r_b^2}\right) - E_i\left(\frac{-r^2}{r_b^2}\,\frac{z_b^2 - i z_b z}{z_b^2 + z^2}\right)\right] \exp(-i\tilde{\psi}_R) \tag{28}$$

where $\alpha_0 = \omega_b r_b / 2c\sqrt{\gamma_0}$ and E_i is the exponential integral function. The derivation of (28) is given in Appendix II. The exponential integral function E_i can be written in series forms (see Appendix III). The amplitude and phase of the *total* field, near the axis $r \leq r_b$, are

$$A_R(r,z) = A_{in} + \alpha_0^2 A_w \left[\left(\tan^{-1}\left(\frac{z}{z_b}\right) + \zeta_i \right) \cos \tilde{\psi}_R \right. \tag{29a}$$

$$\left. - \left(\ln\left(\frac{z^2 + z_b^2}{z_b^2}\right)^{1/2} + \zeta_r \right) \sin \tilde{\psi}_R \right],$$

$$\phi(r,z) = -\alpha_0^2 (A_w/A_R) \left[\left(\tan^{-1}\left(\frac{z}{z_b}\right) + \zeta_i \right) \sin \tilde{\psi}_R \right. \tag{29b}$$

$$\left. + \left(\ln\left(\frac{z^2 + z_b^2}{z_b^2}\right)^{1/2} + \zeta_r \right) \cos \tilde{\psi}_R \right],$$

where $A_{in} = |a_{in}|$, $\zeta_r = \mathrm{Re}(\zeta)$, $\zeta_i = \mathrm{Im}(\zeta)$ and

$$\zeta = \sum_{n=1}^{\infty} \frac{(-1)^n (r/r_b)^{2n}}{n\, n!} \left\{ 1 - \left(\frac{z_b}{z^2 + z_b^2}\right)^n (z_b - iz)^n \right\}.$$

The stationary phase $\tilde{\psi}_R$ is obtained from (12). We notice that in the absence of any efficiency enhancement schemes, the constant resonant phase $\tilde{\psi}_R = -\pi/2$ is stationary. The resonant particle energy also remain constant, see Eq. (27). According to (29a), however, the total radiation field amplitude increases on axis and is given by

$$A_R(r = 0, z) = A_{\text{in}} + \alpha_0^2 A_w \ln\left((z^2 + z_b^2)/z_b^2\right)^{1/2}.$$

The growth of the total radiation field on axis is due to refraction. The index of refraction, in this case, is greater than unity, $n = 1 + (c/\omega)\partial\varphi/\partial z > 1$ over the electron beam, hence the input field tends to focus while the electron beam will defocus. The net radiation energy flux along the z axis (integrated from $r = 0$ to $r = \infty$) is constant (to be shown in the next section), since for large r the radiation amplitude is less than the input amplitude.

V. POWER GAIN AND EFFICIENCY

The increase in total radiation power comes either from the kinetic energy of the electron beam or from the applied D.C. electric field. The increase in the radiation energy flux is

$$\Delta \mathbf{S}_R(x,y,z) = \frac{c(\omega^2/c^2)}{8\pi}\left(a^2(x,y,z) - a^2(x,y,0)\right)\hat{e}_z \tag{30}$$

where $a = a_{in} + a_{ex}$. For the low gain limit, i.e. $|a_{in}| >> |a_{ex}|$,

$$\Delta \mathbf{S}_R = \frac{c(\omega^2/c^2)}{8\pi} A_{in}\,(a_{ex} + a_{ex}^*)\hat{e}_z \tag{31}$$

and total power gain is

$$\Delta P_R(z) = \frac{c}{8\pi}\left(\frac{\omega^2}{c^2}\right) A_{\text{in}} \int_0^\infty \int_0^{2\pi} a_{ex}\, r dr d\theta + \text{c.c.} \tag{32}$$

where a_{ex} is found in Eq. (24). The integrals in Eq. (32) can be evaluated analytically with the following simplifying assumptions: $|\varphi| << 1$, and that $\bar{\gamma}'$ and $\bar{\psi}'$ are independent of transverse coordinates over the cross sectional areas of the electron beam. Furthermore, if r_b satisfies Eqs. (6) and (10) and $k_w r_b << 1$, we can neglect the gradient in the wiggler, and replace $\bar{x}$, $\bar{y}$ in Eq. (32) by x_0, y_0 and $\sigma(v_{y0})$ by $\delta(v_{y0})$. To evaluate Eq. (32), we will write $x = r\cos\theta$, $y = r\sin\theta$, $x_0 = r_0\cos\theta_0$, and $y_0 = r_0\sin\theta_0$. Integrating over all angles, we find that

$$\Delta P_R(z) = -i\,\frac{c}{16\pi}\left(\frac{\omega_b^2}{c^2}\right)\left(\frac{\omega^2}{c^2}\right) A_{\text{in}} \int_0^z dz' \int_0^{2\pi} \frac{d\psi_0}{2\pi} \int_0^\infty r_0 dr_0 \tag{33}$$

$$\int_0^{2\pi} d\theta_0\, \theta(r_0,\theta_0)\, \frac{A_w'}{\bar{\gamma}'} \int_0^\infty r dr\, \frac{e^{i(r^2+r_0^2)\frac{\omega/c}{2(z-z')}}}{z-z'}\, J_0\left(\frac{r r_0 \omega/c}{z-z'}\right) e^{-i\bar{\psi}}.$$

After integrating over all radii, the total power gain given by (33) becomes

$$\Delta P_R = \frac{\omega A_{in}}{8\pi}\,\frac{\omega_b^2}{c^2} \int_0^z dz' \int_0^{2\pi} \frac{d\psi_0}{d\pi}$$

$$\int_{-\infty}^{\infty} dx_0 \int_{-\infty}^{\infty} dy_0\, \theta(x_0,y_0)\, \frac{A_w'}{\tilde{\gamma}'} \cos \tilde{\psi}'. \tag{34}$$

For a Gaussian beam profile for the electron beam, i.e., $\theta(x_0,y_0) = \exp - (x_0^2 + y_0^2)/r_b^2$, and assuming that all the particles have the same stationary resonant phase $\tilde{\psi}_R$, the total power gain is

$$\Delta P_R = \frac{c(\omega/c)}{8\pi} \frac{\omega_b^2}{c^2} \pi r_b^2 \frac{A_w A_{in}}{\gamma_R} z \cos \tilde{\psi}_R. \tag{35}$$

Let us apply ΔP_R to $\cos \tilde{\psi}_R = 0$ ($\tilde{\psi}_R = -\pi/2$), for which case the electrons do not lose any kinetic energy. Even though the radiation amplitude grows on axis, the total radiation energy flux is constant $\Delta P_R = 0$, consistent with the fact that electrons remains at the same kinetic energy. The increase in the radiation amplitude on axis is due to refraction effects at the expense of a corresponding decrease in the off axis radiation field.

To complete our formulation of the FEL, we need an expression for the efficiency,

$$\eta = \frac{\Delta P_R}{v_{z0}\, n_0 (\gamma_0 - 1) m_0 c^2 \int_{-\infty}^{\infty} dx_0 \int_{-\infty}^{\infty} dy_0\, \theta(x_0,y_0)}. \tag{36}$$

If a D.C. electric field is applied for efficiency enhancement, the trapped electrons do not change their kinetic energy. The radiation power gain, in this case, originates from the energy flux due to the D.C. electric field crossed with the self-magnetic field, i.e., $-\frac{\partial \phi_{DC}}{\partial z}\, \hat{e}_z \times \mathbf{B}_{self}$, which is in the radial direction flowing inward toward the electron beam.

The electric field required to maintain a stationary resonant phase $\tilde{\psi}_R$, based on Eq. (27), is

$$\frac{\partial \phi_{DC}}{\partial z} = \frac{1}{2} \left(\frac{|e|}{m_0 c^2} \right) \frac{\omega/c}{\gamma_R} A_w A_R (r = 0,\, z) \cos \tilde{\psi}_R.$$

For a resonant macro particle, the efficiency can also be written as

$$\eta = |e| \left(\phi_{DC}(z) - \phi_{DC}(0)\right)/\gamma_0 m_0 c^2$$

or

$$\eta = -\left(\frac{|e|}{m_0 c^2} \right)^2 \frac{\omega/c}{2\gamma_0^2} \int_0^z A_w A_R (r = 0, z') \cos \tilde{\psi}_R\, dz', \tag{37}$$

which is the same as Eq. (36) together with Eq. (35).

VI. NUMERICAL EXAMPLE

As an example of a 10.6 μm FEL utilizing a CO_2 laser as an input field, we choose an electron beam of energy 25 MeV ($\gamma_0 = 50$), current of $I = 5$ A and radius (Gaussian profile) of $r_b = 0.5$ mm. Such a beam has a peak density on axis of $n_0 = 1.3 \times 10^{11}$ cm^{-3} ($\omega_b = 2.0 \times 10^{10}$ sec^{-1}). The constant parameter wiggler has a magnitude of $B_w = 5.0$ kG and wavelength of $l_w = 2.8$ cm which gives $A_w = 2.2 \times 10^3$ statvolts. The wiggle velocity is $v_{0\perp} = 2.6 \times 10^{-2}c$ and the input CO_2 power density is taken to the $P_{in} = 4 \times 10^8$W/cm^2 which gives $A_{in} = 0.30$ statvolts. Note that the inequalities in (3) and (10) are well satisfied.

Our first illustration makes the resonant macro particle approximation and is one in which the applied D.C. electric potential is zero, hence, $\tilde{\psi}_R = -\pi/2$ and the particle energy remains constant. The curves in Figs. 3a,b and 4a,b are the numerical results of Eq. (28). Figure 3a shows the gain,

$$G(r,z) = (A_R(r,z) - A_{in})/A_{in} \tag{38}$$

as a function of radius at $z = 20$ cm, 1 m and 2 m; and Fig. 3b shows the gain as a function of axial position z at various radial positions, i.e., $r = 0$, $r = r_b$, $r = 3r_b$ and $r = 5r_b$. The gain in the radiation amplitude at $z = 2$ m is maximum on axis and equal to 0.14.

Figure 4a shows the radial cross section of total radiation phase φ at $z = 20$ cm, 1 m and 2 m; and Fig. 4b shows the total radiation phase φ as a function of axial position at various radial positions. The maximum value of φ is along the z axis and is approximately 0.06 rad which certainly satisfies our approximation used in (25) to obtain (28). The index of refraction, in this case, is greater than unity, $n = 1 + (c/\omega)\partial\varphi/\partial z > 1$ over the electron beam, hence the input field tends to focus while the electron beam will defocus. The net radiation energy flux along the z axis (integrated from $r = 0$ to $r = \infty$) is constant, since for large r the radiation amplitude is less than the input amplitude.

Our next illustration still assumes resonant macro particles, but will include an applied D.C. electric potential $\phi_{DC}(z)$ such that $\cos\tilde{\psi}_R = 0.6$. Figures 5 a,b and 6 a,b are the numerical results of Eq. (28) for this example. The gain in radiation amplitude on axis at $z = 2$ m is 0.15, see Fig. 5. The efficiency at the end of $z = 2$ m is $\sim$3.6%. Figure 6a shows the phase φ as a function of radius, and Fig. 6b shows the phase φ as a function of z. For large z, n is less than unity on axis (defocusing) and becomes greater than unity for large r (focusing).

For our last example, we will not apply the stationary resonant phase approximation. Instead we take the electrons to enter the interaction region with a uniform distribution in initial phase ψ_0. The wiggler amplitude is tapered to enhance the efficiency, $B_w(z) = B_w(0)(1 - \alpha z)$, where $\alpha = 0.0003$ cm^{-1}. The form of the applied wiggler field is such that one particle is maintained at approximately constant phase,

$$\cos\psi_R = -(2k_w A_R)^{-1}\frac{dA_w}{dz} = 0.5.$$

Figure 7 is a plot of gain calculated from (26) as a function of axial position for $r = 0$, $r = r_b$ and $r = 3\ r_b$. The oscillations are due to the particles bouncing in the ponderomotive potential wells. The efficiency as a function of z, Eq. (36), is plotted in Fig. 8.

ACKNOWLEDGMENT

The authors appreciate useful discussions with I.B. Bernstein. The authors would also like to acknowledge support for this work by DARPA under Contract No. 3817.

REFERENCES

1. J.M.J. Madey, J. Appl. Phys. **42**, 1906 (1971).

2. P. Sprangle and V.L. Granatstein, Appl. Phys. Lett. **25**, 377 (1974).

3. W.B. Colson, Phys. Lett. A, **64**, 190 (1977).

4. P. Sprangle, R.A. Smith and V.L. Granatstein, NRL Report No. 3911 (1978) and *Infrared and Millimeter Waves*, Edited by K. Button (Academic Press, New York, 1979), Vol. 1.

5. N.M. Kroll and W.A. McMullin, Phys. Rev. A **17**, 300 (1978).

6. P. Sprangle and A.T. Drobot, J. Appl. Phys. **50**, 2652 (1979).

7. P. Sprangle, Cha-Mei Tang and W.M. Manheimer, Phys. Rev. Lett. **43**, 1932 (1979) and Phys. Rev. A **21**, 302 (1980).

8. P. Sprangle and Cha-Mei Tang, Proc. 4th Int'l Conf. on Infrared and Near Millimeter Waves, S. Perkowitz, Ed., Miami Beach, 10-15 Dec 1979, p.98.

9. P. Sprangle and R.A. Smith, NRL Memorandum Report No. 4033 (1979) and Phys. Rev. A **21**, 293 (1980).

10. *Free-Electron Generators of Coherent Radiation*, Physics of Quantum Electronics, Vol. 7, (1980), Edited by S.F. Jacobs, H.S. Pilloff, M. Sargent III, M.O. Scully and R. Spitzer, Addison-Wesley Publishing Co.

11. N.M. Kroll, P. Morton and M.N. Rosenbluth, JASON Tech. Report JSR-97-15, 1980.

12. A.T. Lin and J.M. Dawson, Phys. Rev. Lett. **42**, 1670 (1979).

13. L. Friedland and J.L. Hirshfield, Phys. Rev. Lett. 44, 1456 (1980).

14. Cha-Mei Tang and P. Sprangle J. Appl. Phys. 52, 3148 (1981).

15. 3-D effects in the FEL were first discussed by i) J. Slater, DARPA FEL Review, Arlington, Va., Dec. 3-4, 1979,ii) P. Sprangle and Cha-Mei Tang, DARPA/ONR/AFOSR FEL Program Review, LASL, April 24-25, 1980, and iii) Y.P. Ho, Y.C. Lee and M.N. Rosenbluth, Sherwood Meeting, Tucson, Arizona, April 23-25, 1980.

16. P. Sprangle and Cha-Mei Tang, Applied Phys. Lett. 39, 677 (1981); P. Sprangle and Cha-Mei Tang, AIAA Journal, 19, 1164 (1981); Cha-Mei Tang and P. Sprangle, Proceedings of the Int'l Conf. on Laser's 80, STS Press, McLean, Va., 13 (1981).

17. J.M. Slater and D.D. Lowenthal, "Diffraction Effects in Free Electron Lasers", Math Science North West (1980).

18. C. James Elliott, "Transverse Optical Effects", LASL, Private communications (1980).

19. L.R. Elias and J.C. Gallardo, "Coherent Lienard-Wiechent Fields Produced by Free Electron Laser," Quantum Institute Report QIFEL-009/81, Univ. of California, Santa Barbara, CA. 93106 (1981).

20. D. Prosnitz, R.A. Haas, S. Doss and R.J. Gelinas, "Two-Dimensional Numerical Model of a Free Electron Laser Amplifier," Conf. on Lasers and Electro-Optics, Washington, D.C., June 10-12, 1981, and ONR Workshop on FEL, Sun Valley, Idaho, June 22-25, 1981.

Appendix I

BETATRON OSCILLATIONS DUE TO TRANSVERSE GRADIENT OF THE WIGGLER FIELD

This appendix will obtain the particle's transverse motion (5a) and the axial velocity spread (7) inside a linearly polarized realizable wiggler field. For the illustrative purposes here, we will assume that the wiggler amplitude and wavelength are constant in the axial direction. The vector potential of the wiggler field is

$$\mathbf{A}_w(y,z) = A_w \cosh(k_w y) \cos(k_w z)\, \hat{e}_x. \tag{I.1}$$

The associated wiggler magnetic field has a z component off the axis, in addition to the y component,

$$\mathbf{B}_w(y,z) = {}^{-}A_w k_w [\cosh(k_w y) \sin(k_w z)\, \hat{e}_y + \sinh(k_w y) \cos(k_w z)\, \hat{e}_z]. \tag{I.2}$$

For particle trajectories in the transverse directions, it is sufficient to assume that their motion is effected by the wiggler field alone, i.e., $\mathbf{P}_x(y,z) \simeq \frac{|e|}{c}\mathbf{A}_w$.

The particle location in the x-direction can be obtained by integrating the momentum in the x direction.

$$\bar{x} = x_0 + \frac{\beta_{\alpha}}{k_w} \cosh(k_w \bar{y}) \sin k_w z \tag{I.3}$$

where $\bar{x}$ and $\bar{y}$ are functions of $(z, \psi_0, x_0, y_0, v_{y_0})$, x_0 and y_0 are the initial transverse coordinates, v_{y_0} is the initial transverse velocity in the y-direction, and ψ_0 is the initial phase of the electron in the ponderomotive potential well at the entrance to the interaction region, i.e., $z = 0$.

The particle motion in the y-direction is due to the z component of the wiggler field,

$$\frac{dP_y}{dt} = \frac{|e|}{c} v_x B_z. \tag{I.4}$$

We will assume that the fast oscillatory terms, with wavelength half the wiggler wavelength, are unimportant (see Ref. (14)), and replace v_z by c at appropriate places. We find that

$$\frac{d^2y}{dz^2} + \frac{\beta_{\alpha\perp}^2}{4} k_w \sinh 2k_w y = 0 \tag{I.5}$$

where $\beta_{\alpha\perp} = |e|A_w/(\gamma_0 m_0 c^2)$. This equation can be integrated once to give

$$\frac{dy}{dz} = \left[\frac{\beta_{\alpha\perp}^2}{4} (\cosh(2k_w y_0) - \cosh(2k_w y)) + (\frac{v_{y_0}}{c})^2\right]^{1/2}. \tag{I.6}$$

To find an explicit solution of y as a function of z, we expand cosh in Taylor series around zero, and keep only the first two terms of the expansion. Then, Eq. (I.6) can be rewritten as

$$z = \frac{\sqrt{2}}{\beta_{\alpha\perp} k_w} \int_{y_0}^{y} \left[2\left(\frac{v_{y_0}/c}{\beta_{\alpha\perp} k_w}\right)^2 + y_0^2 - y^2\right]^{1/2}. \tag{I.7}$$

The results of the integral can be put into the following form

$$\begin{bmatrix} \tilde{y} \\ \tilde{v}_y \end{bmatrix} = \begin{bmatrix} \cos K_0 z & (K_0 c)^{-1} \sin K_0 z \\ -K_0 c \sin K_0 z & \cos K_0 z \end{bmatrix} \begin{bmatrix} y_0 \\ v_{y_0} \end{bmatrix} \tag{I.8}$$

where $K_0 = \beta_{\alpha\perp} k_w/\sqrt{2}$ is the wavenumber of the betatron oscillations. An equally convenient form for $\tilde{y}$ is

$$\tilde{y} = y_B \cos(K_0 z - \phi_B) \tag{I.9}$$

where

$$y_B = \left[2\left(\frac{v_{y_0}/c}{\beta_{\alpha\perp} k_w}\right)^2 + y_0^2\right]^{1/2} \tag{I.10}$$

is the amplitude of the betatron oscillation and

$$\phi_B = \cos^{-1}(y_0/y_B) \tag{I.11}$$

is the initial phase of the betatron oscillation.

We will now show that the axial velocity of the particles decrease as the amplitude of the betatron oscillations increase. This results in an equivalent energy spread. For illustrative purposes, we will consider a cold electron beam with total energy $\gamma_0 m_0 c^2$. The axial velocity is found to be

$$\left(\frac{v_z}{c}\right)^2 = \frac{\gamma_0^2 - 1}{\gamma_0^2} - \beta_{\alpha\perp}^2 [\cosh^2(k_w y) \cos^2(k_w z) + 1/4(\cosh(2k_w y_0) - \cosh(2k_w y))] - \left(\frac{v_{y_0}}{c}\right)^2. \tag{I.12}$$

In the derivation of (I.12), we have used $v_y/c = dy/dz$ from (I.6) and $v_x/c = P_x/(\gamma_0 m_0 c)$. We will again drop terms that oscillate at twice the wiggler wavenumber. We obtain $v_z = v_{z0} - \Delta v_z$, where $v_{z_0} = v_0 - \beta_{\perp}^2 c/4$ (the mean axial velocity in the absence of the betatron oscillation in a non-realizable wiggler field without transverse gradient) is the axial velocity of the electron travelling on axis in a realizable wiggler field, and $\Delta v_z = c(\beta_{\perp} k_w y_B/2)^2$ is the amount that the axial velocity is reduced by for particles executing betatron oscillations with oscillation amplitude y_B. Since the axial velocity spread is proportional to the radial excursion, the maximum axial velocity spread, due to betatron oscillation alone, is

$$\Delta v_z = c(\beta_{\perp} k_w r_b/2)^2 \tag{I.13}$$

where r_b is the radius of the electron beam.

Appendix II

DERIVATION OF THE EXCITED RADIATION FIELD IN THE RESONANT PARTICLE LIMIT

The details of the derivation of the excited resonant particle radiation field, Eq. (28), will be given here. The excited radiation field, for the electron beam with all initial phase ψ_0, is given by (25). In the constant phase, resonant particle limit,

$$\int_0^{2\pi} \frac{d\psi_0}{2\pi} e^{-i\tilde{\psi}(z',\psi_0)} = e^{-i\tilde{\psi}_R}$$

where all the particles have the same phase $\tilde{\psi}_R$. We can now rewrite (25) as

$$a_{ex}(r,z) = -i\alpha_0^2 A_w \, I(r,z) e^{-i\tilde{\psi}_R}, \tag{II.1}$$

where

$$I(r,z) = \int_0^z dz' \left[\frac{(z-z') + iz_b}{(z-z')^2 + z_b^2}\right] \exp\left[iz_b \frac{r^2}{r_b^2}\left(\frac{z - z' + iz_b}{(z - z')^2 + z_b^2}\right)\right], \tag{II.2}$$

and $\alpha_0 = \omega_b r_b/(2c\sqrt{\gamma_0})$. The integral (I.2) can be rearranged into the following form

$$I = -i\frac{r_b^2}{z_b} \frac{\partial}{\partial r^2} \int_0^z dx \exp\left[i \frac{r^2}{r_b^2}\left(\frac{z_b}{x-iz_b}\right)\right] \tag{II.3}$$

where $x = z - z'$. We make another change of variables, $q = -iz_b/(x-iz_b)$, and we find

$$I = -\int_1^{-i\frac{z_b}{z-iz_b}} f\left(\frac{r^2}{r_b^2},q\right) dq \tag{II.4}$$

where

$$f(b,q) = \frac{1}{q} \exp(-bq). \tag{II.5}$$

Since the function $f(b,q)$ satisfies the Cauchy-Riemann condition, we can evaluate the integral in (II.4) by changing the contour of integration to that below

$$I = -\int_1^{\infty} f\left(\frac{r^2}{r_b^2},q\right) dq - \int_{\infty}^{\frac{-iz_b}{z-iz_b}} f\left(\frac{r^2}{r_b^2},q\right) dq. \tag{II.6}$$

Let $p = \dfrac{z - iz_b}{-iz_b}\, q$ in the second integral, we can rewrite (II.6) as

$$I = -\int_1^{\infty} f\left(\frac{r^2}{r_b^2}, q\right) dq + \int_1^{\infty} f\left(\frac{r^2}{r_b^2}\, \frac{z_b(z_b - iz)}{z_b^2 + z^2}, p\right) dp \tag{II.7}$$

Since

$$E_i(-b) = -\int_1^{\infty} f(b,q)\, dq, \tag{II.8}$$

we obtain (28),

$$a_{ex}\,(r,z) = -i\alpha_0^2 A_w \left[E_i\left(\frac{-r^2}{r_b^2}\right) - E_i\left(\frac{-r^2}{r_b^2}\left(\frac{z_b^2 - iz_b z}{z_b^2 + z^2}\right)\right)\right] \exp\,(-i\bar{\psi}_R), \tag{II.9}$$

where E_i is the exponential integral function.

Appendix III

THE AMPLITUDE AND PHASE OF THE TOTAL FIELD IN THE RESONANT PARTICLE LIMIT

This appendix will derive the amplitude and phase of the total field (Eqs. (29a, b)) from the excited radiation field, (Eq. (28)). The complex amplitude of excited radiation field can be written as

$$a_{ex}(r,z) = -\, i\alpha_0^2 A_w \, I(r,z) \exp\,(-i\tilde{\psi}_R) \tag{III.1}$$

where

$$I = E_i\left(-\frac{r^2}{r_b^2}\right) - E_i\left(-\frac{r^2}{r_b^2}\,\frac{z_b^2 - iz_b z}{z_b^2 + z^2}\right), \tag{III.2}$$

$\alpha_0 = \omega_b r_b/(2c\sqrt{\gamma_0})$, and E_i is the exponential integral function. The function can be evaluated using the series representation

$$E_i(x) = C + \ln\,(-x) + \sum_{n=1}^{\infty} \frac{x^n}{nn!} \qquad (x < 0) \tag{III.3}$$

where C is the Euler's constant. Applying (III.3) to (III.2), we obtain

$$I = \ln\left(\frac{z^2 + z_b^2}{z_b^2}\right)^{1/2} + i\,\tan^{-1}\left(\frac{z}{z_b}\right) \tag{III.4}$$

$$+ \sum_{n=1}^{\infty} \frac{(-1)^n (r/r_b)^{2n}}{nn!}\left[1 - \left(\frac{z_b}{z^2 + z_b^2}\right)^n (z_b - iz)^n\right].$$

when $r^2/r_b^2 >> 1$, an asymptotic expansion for E_i is more appropriate,

$$E_i\,(-\xi) = -\frac{e^{-\xi}}{\xi}\left(1 - \frac{1}{\xi} + \frac{2!}{\xi^2} - \frac{3!}{\xi^3} + \ldots\right) \qquad [\xi >> 1]. \tag{III.5}$$

The asymptotic expansion for (III.2) becomes

$$I = -\frac{\exp\,(-r^2/r_b^2)}{r^2/r_b^2}\left[1 + \sum_{n=1}^{\infty} \frac{(-1)^n\, n!}{(r/r_b)^{2n}}\right] \tag{III.6}$$

$$+ \frac{\exp\,(-p)}{p}\left[1 + \sum_{n=1}^{\infty} \frac{(-1)^n\, n!}{p^n}\right]$$

where

$$p = \left(\frac{z_b}{z_b + iz}\right)\left(\frac{r^2}{r_b^2}\right).$$

We have defined

$$a_R = A_R e^{i\varphi} = a_{in} + a_{ex}$$

where a_R is the complex amplitude of the total radiation field, A_R and φ are the amplitude and phase of the total radiation field, $a_{in} = A_{in}$ is the amplitude of the input radiation field. In the limit that $|\varphi| << 1$, we can write

$$A_R = A_{in} + \alpha_0^2\, A_w\, [I_i \cos \bar{\psi}_R - I_r \sin \bar{\psi}_R] \tag{III.7a}$$

$$\varphi = -\alpha_0^2\, \frac{A_w}{A_R}\, [I_i \sin \psi_R + I_r \cos \bar{\psi}_R] \tag{III.7b}$$

where $I_r = \mathrm{Re}(I)$, $I_i = \mathrm{Im}(I)$. For $r^2/r_b^2 \leq 1$, A_R and φ can be rewritten as (29a, b).

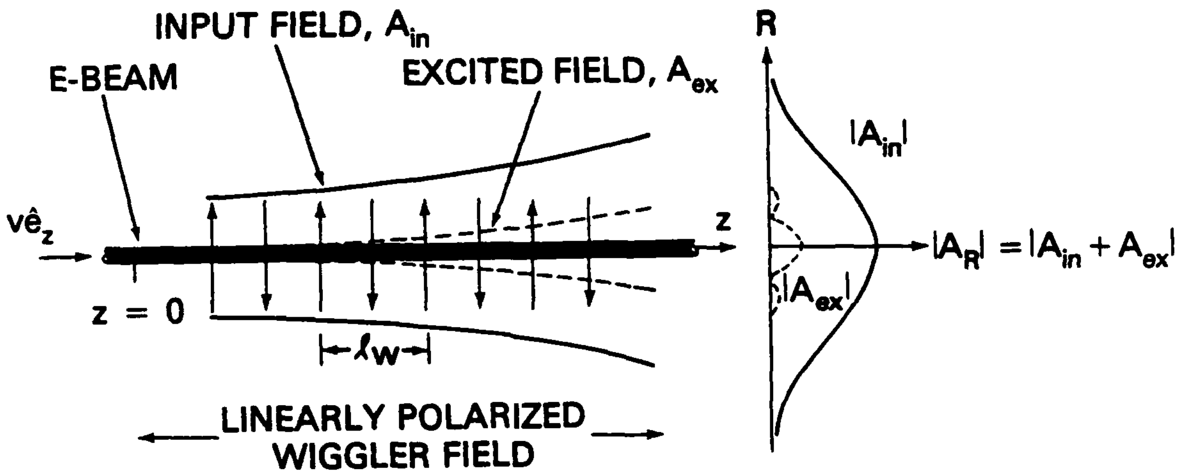

Fig. 1 — Schematic of electron and radiation beams in 3-D FEL amplifier configuration.

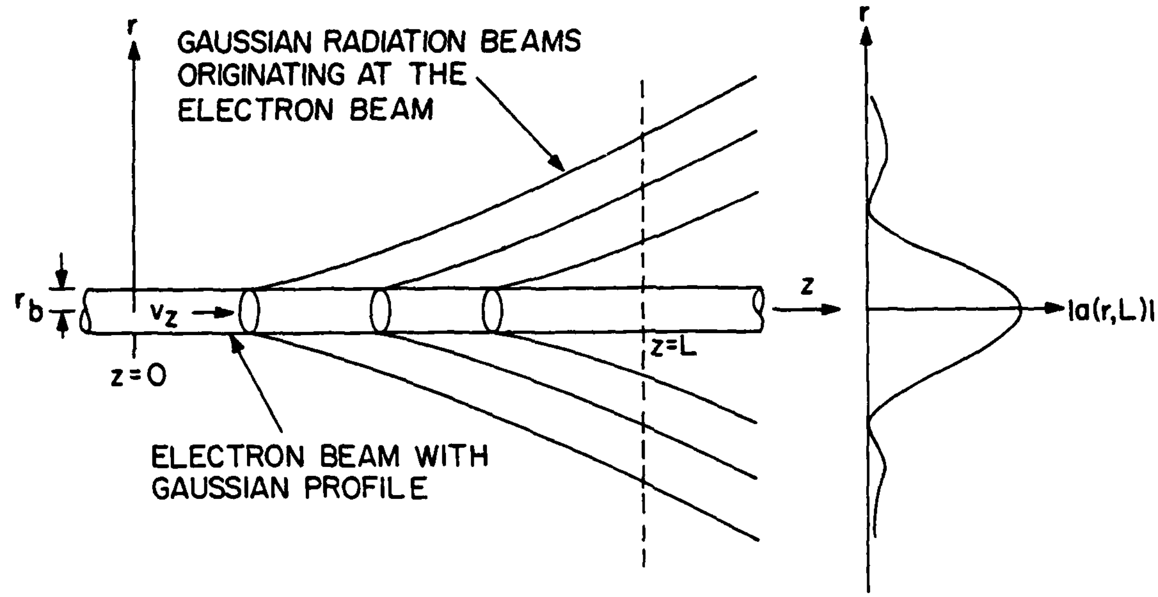

Fig. 2 — Schematic interpretation of the excited radiation. Gaussian like TEM_{00} radiation beams with the minimum spot size equal to the electron beam radius are continuously produced at each cross section of the electron beam. The total excited radiation at a location $z = L$ down stream is the sum of all the Gaussian radiation beams which originated from $z = 0$ to $z = L$.

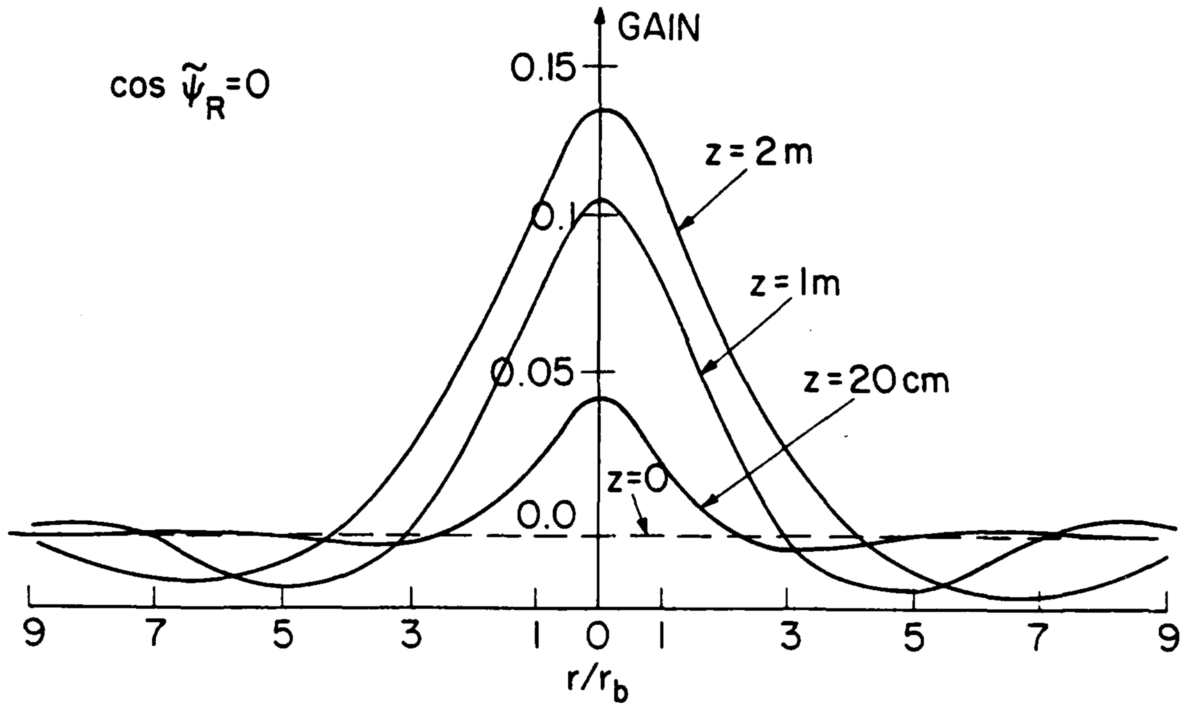

Fig. 3a — Gain as a function of radius at z = 20cm, 1m and 2m for resonant macro particles with cos $\tilde{\psi}_r$ = 0.

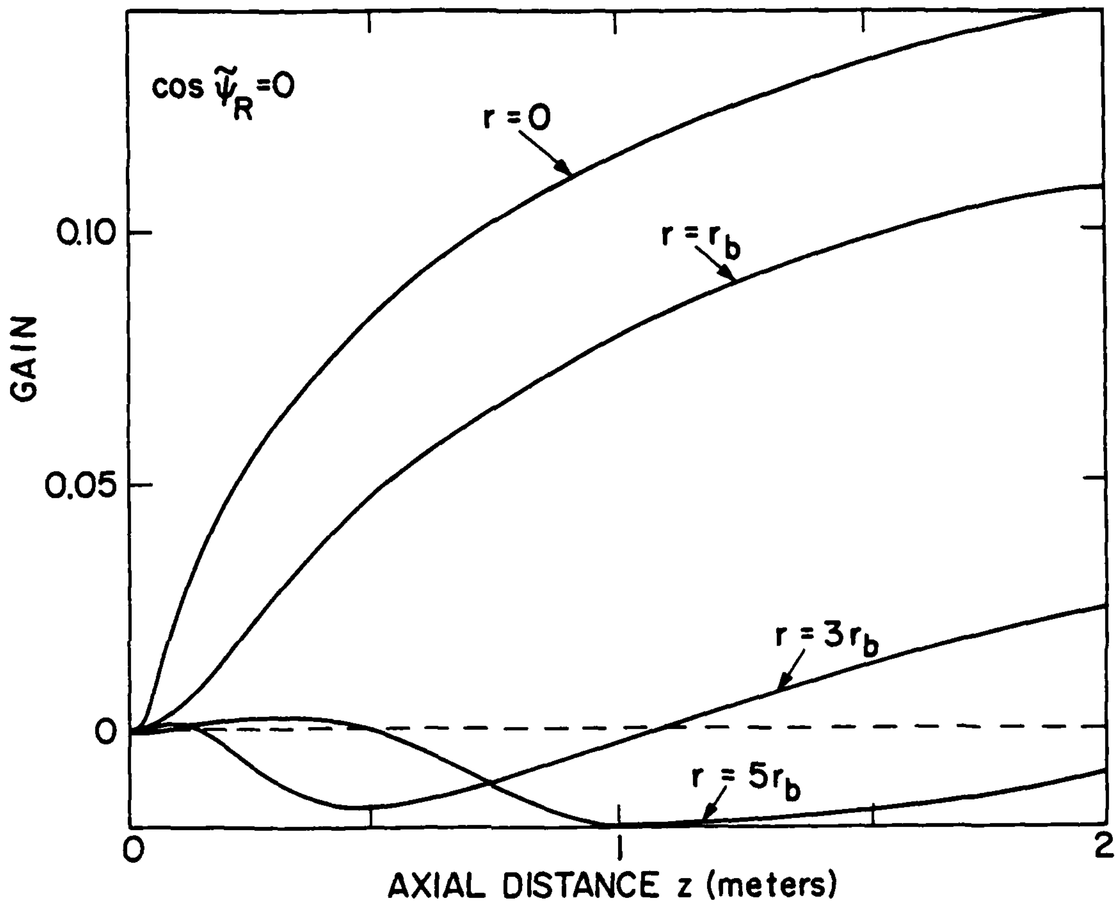

Fig. 3b — Gain as a function of z at various radial positions for resonant macro particles with cos $\tilde{\psi}_R$ = 0.

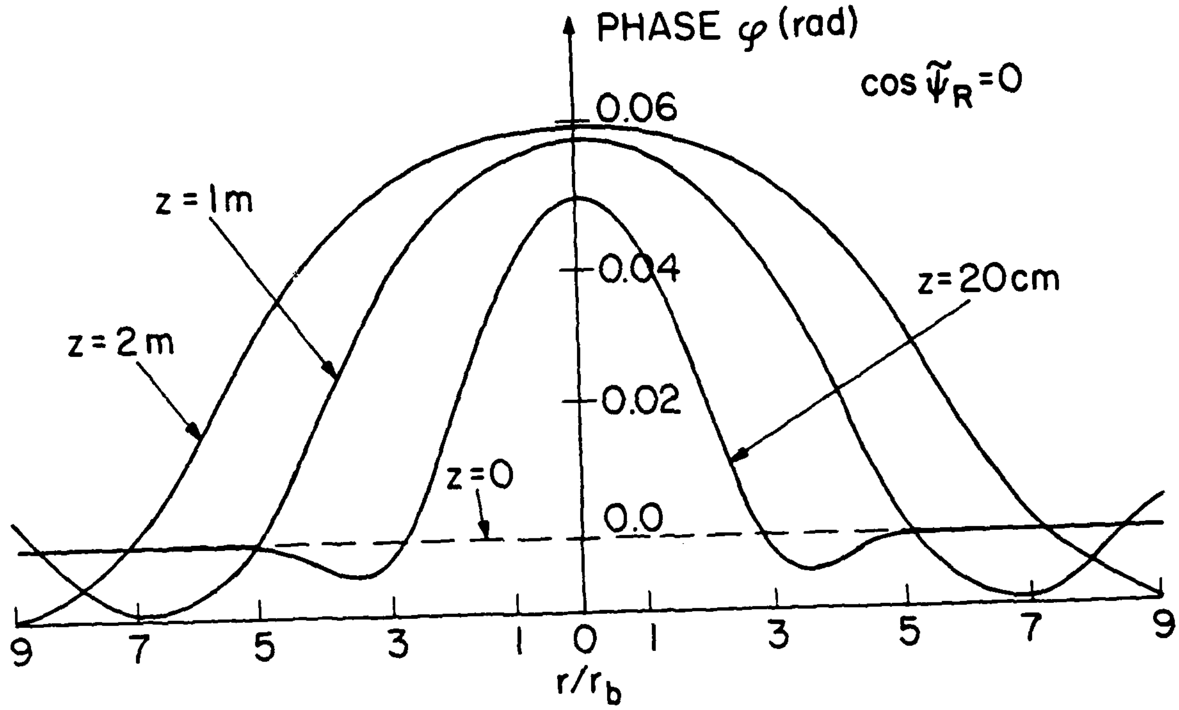

Fig. 4a — Total radiation phase, φ, as a function of radius at z = 20cm, 1m and 2m for resonant macro particles with $\cos \tilde{\psi}_R = 0$.

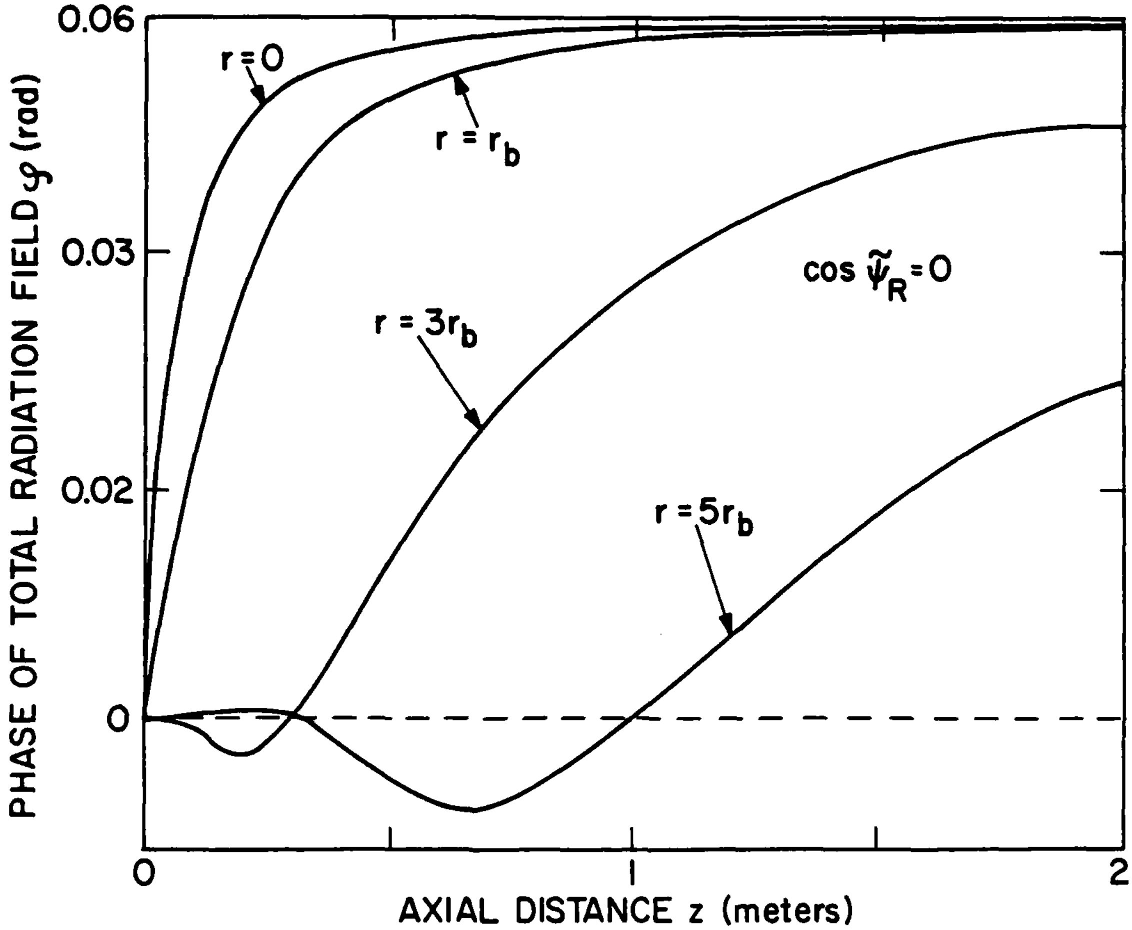

Fig. 4b — Total radiation phase, φ, as a function of z at various radial positions for resonant macro particles with $\cos \tilde{\psi}_R = 0$.

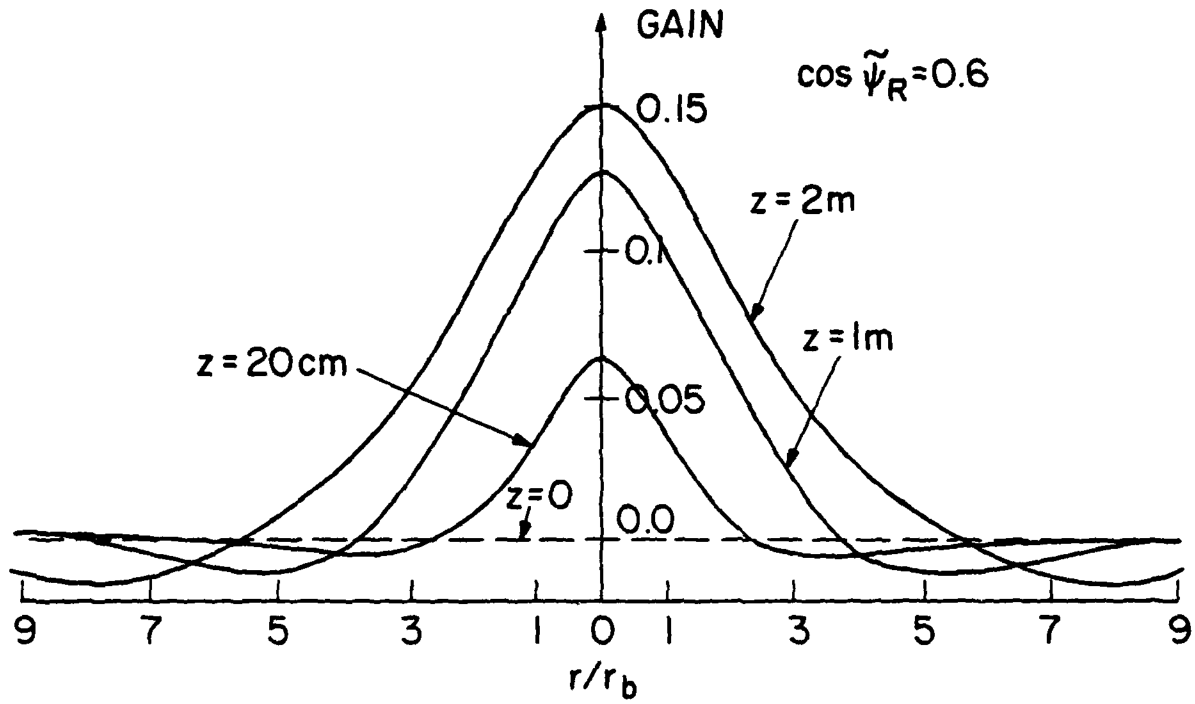

Fig. 5a — Gain as a function of radius at z = 20cm, 1m and 2m for resonant macro particles with $\cos \tilde{\psi}_R$ = 0.6.

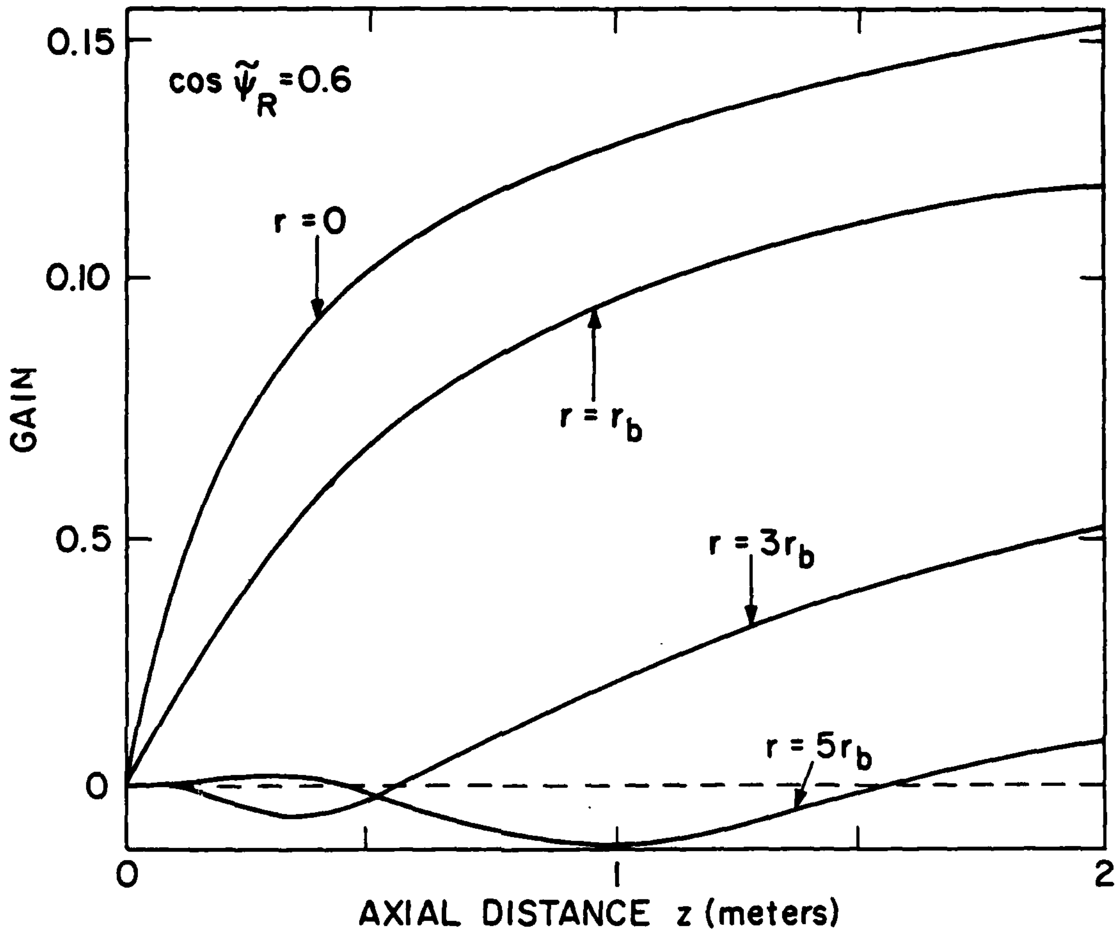

Fig. 5b — Gain as a function of z at various radial positions for resonant macro particles with $\cos\tilde{\psi}_R = 0.6$.

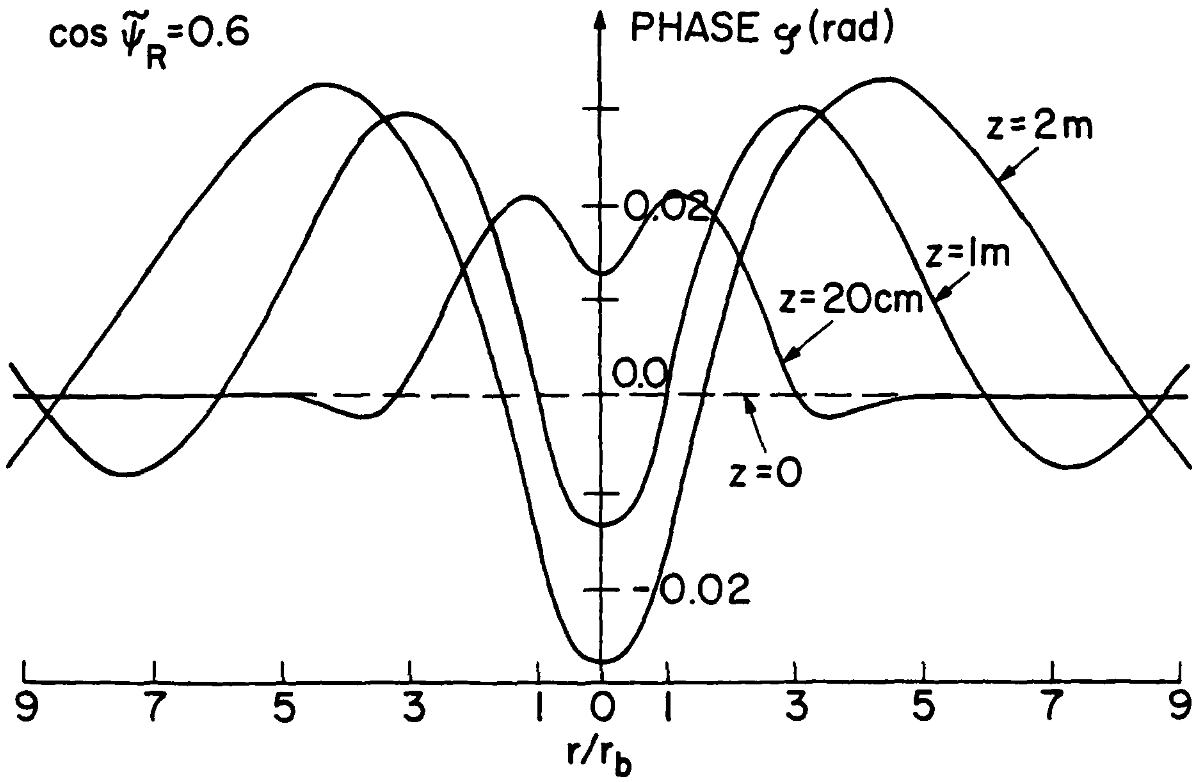

Fig. 6a — Total radiation phase, φ, as a function of radius at z = 20cm, 1m and 2m for resonant macro particles with $\cos\tilde{\psi}_R$ = 0.6.

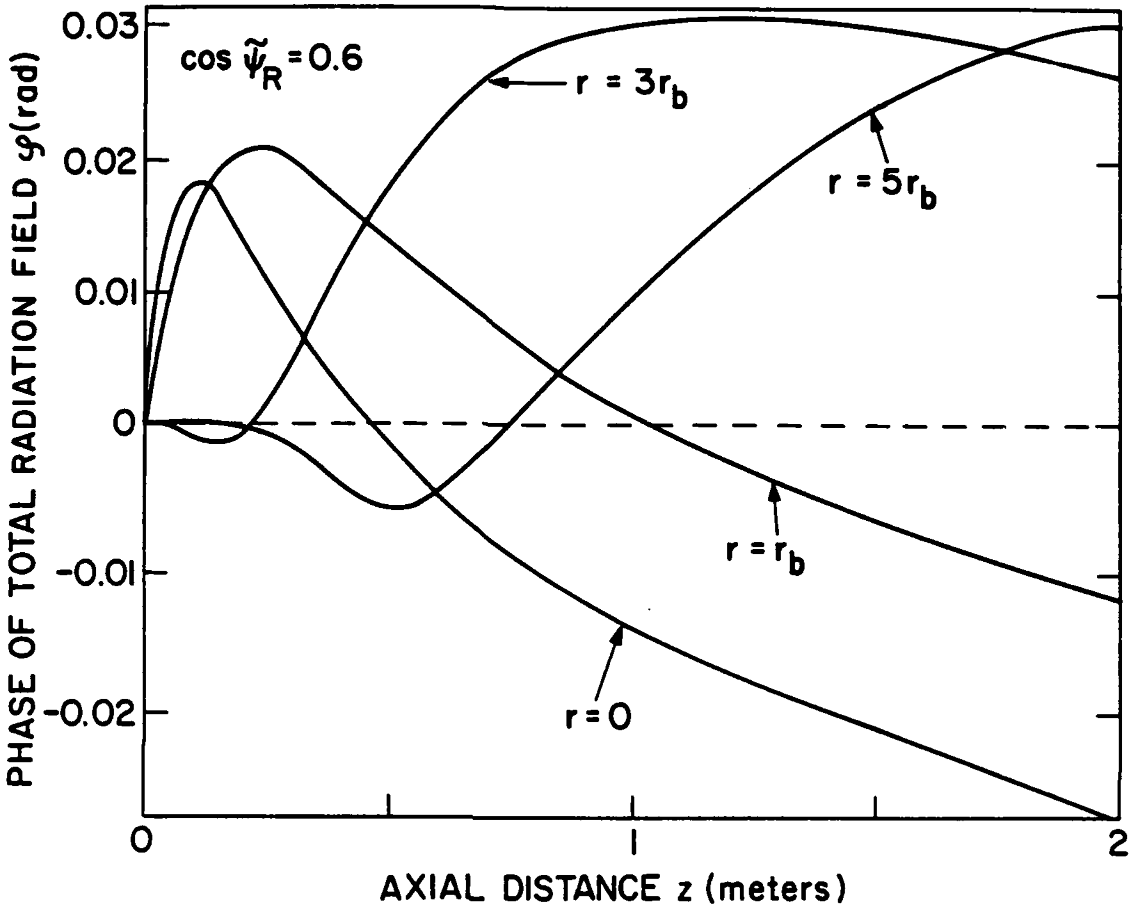

Fig. 6b — Total radiation phase, φ, as a function of z at various radial positions for resonant macro particles with $\cos \tilde{\psi}_R = 0.6$.

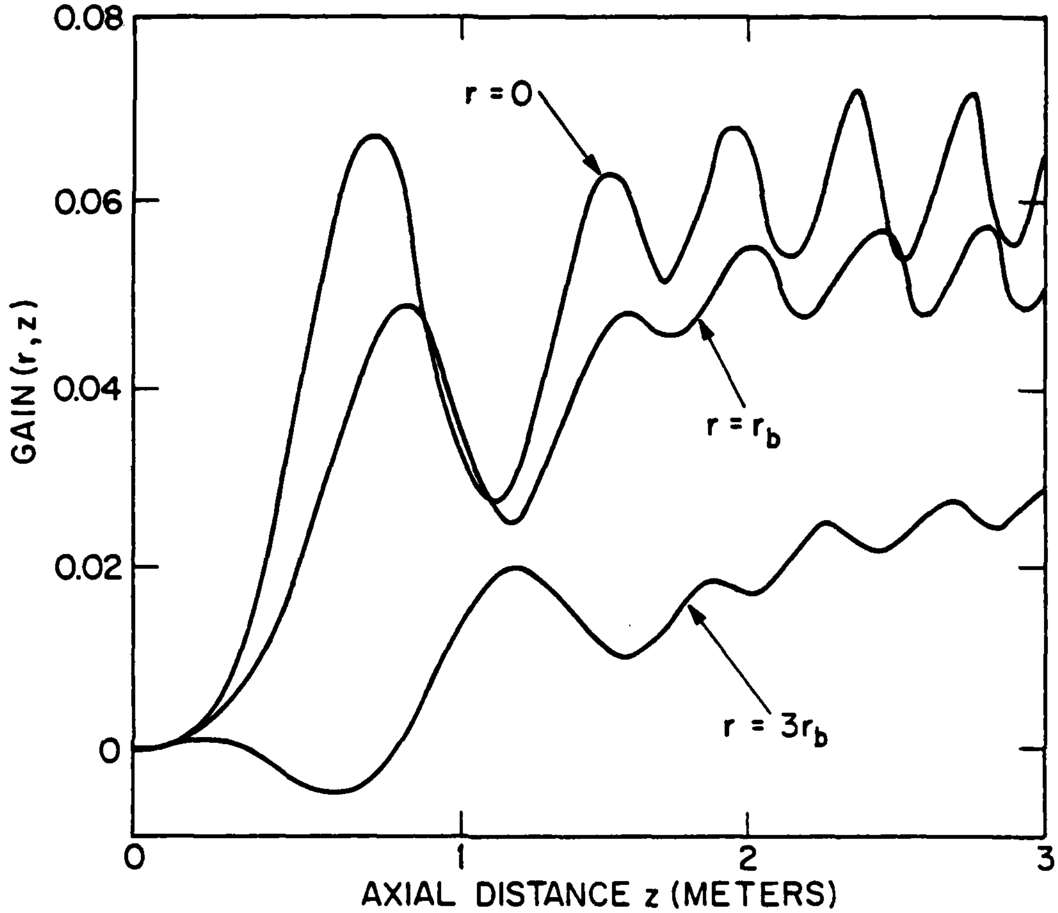

Fig. 7 — Gain as a function of z at $r = 0$, $r = r_b$ and $r = 3r_b$ for electron beam with uniform distribution of initial phase ψ_0 in a tapered wiggler field.

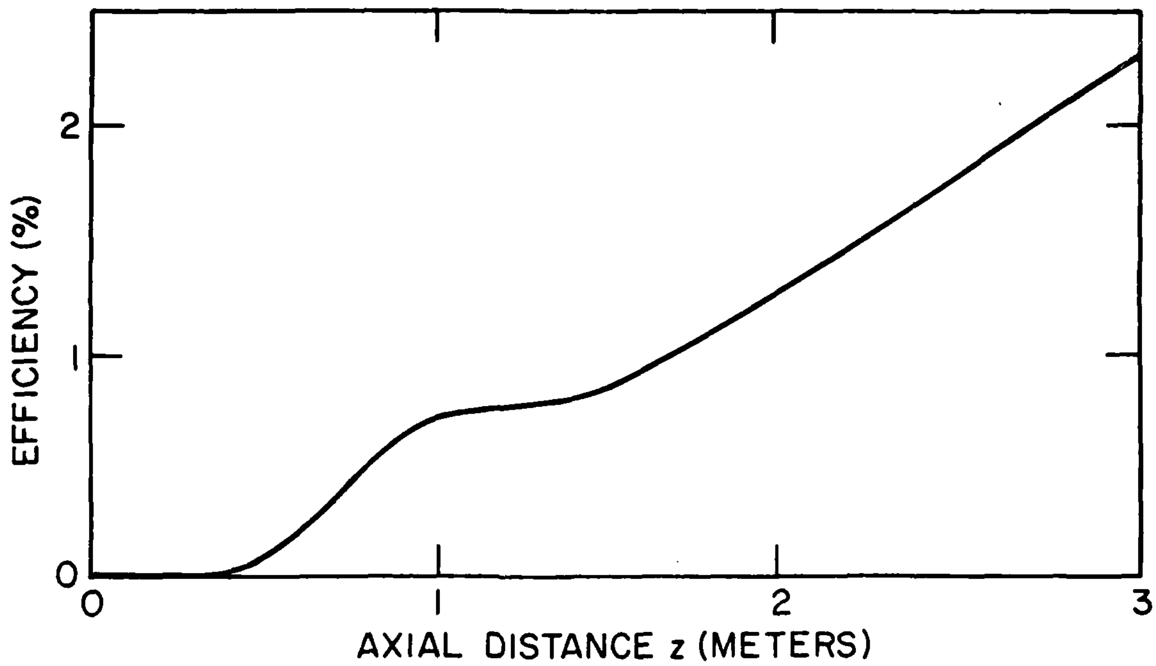

Fig. 8 — Efficiency as a function of z for electron beam with uniform distribution of initial phase ψ_0 in a tapered wiggler field.

DISTRIBUTION LIST*

Naval Research Laboratory
4555 Overlook Avenue, S.W.
Washington, D.C. 20375

Attn: Code 1000 - CAPT. E. E. Henifin
1001 - Dr. A. Berman
4700 - Dr. T. Coffey (26 copies)
4701 - Mr. J. Brown
4740 - Dr. V. L. Granatstein (20 copies)
4740 - Dr. K. R. Chu
4740 - Dr. C. W. Roberson
4790 - Dr. P. Sprangle (100 copies)
4790 - Dr. C. M. Tang
4790 - Dr. M. Lampe
4790 - Dr. W. M. Manheimer
6603S- Dr. W. W. Zachary
6650 - Dr. L. Cohen
6656 - Dr. N. Seeman
6850 - Dr. L. R. Whicker
6805 - Dr. S. Y. Ahn
6805 - Dr. R. K. Parker (20 copies)
6875 - Dr. R. Wagner

On Site Contractors:
Code 4740 - Dr. L. Barnett (B-K Dynamics)
4740 - Dr. D. Dialetis (SAI)
4740 - Dr. Y. Y. Lau (SAI)
4790 - Dr. A. T. Drobot (SAI)
4790 - Dr. J. Vomvoridis (JAYCOR)
4790 - Dr. H. Freund (SAI)

* Every name listed on distribution gets one copy except for those where extra copies are noted.

Dr. Tony Armstrong
SAI, Inc.
P. O. Box 2351
La Jolla, CA 92038

Dr. Robert Behringer
ONR
1030 E. Green
Pasadena, CA 91106

Dr. G. Bekefi (5 copies)
Massachusetts Institute of Technology
Bldg. 26
Cambridge, MA 02139

Dr. Arden Bement (2 copies)
Deputy Under Secretary of Defense
for R&AT
Room 3E114, The Pentagon
Washington, D.C. 20301

Lt Col Rettig P. Benedict Jr., USAF
DARPA/STO
1400 Wilson Boulevard
Arlington, VA 22209

Dr. T. Berlincourt
Code 420
Office of Naval Research
Arlington, VA 22217

Dr. I. B. Bernstein (2 copies)
Yale University
Mason Laboratory
400 Temple Street
New Haven, CT 06520

Dr. Charles Brau (2 copies)
Applied Photochemistry Division
Los Alamos National Scientific
Laboratory
P. O. Box 1663, M.S. - 817
Los Alamos, NM 87545

Dr. R. Briggs (L-71)
Lawrence Livermore National Lab.
P. O. Box 808
Livermore, CA 94550

Dr. Fred Burskirk
Physics Department
Naval Postgraduate School
Monterey, CA 93940

Dr. K. J. Button
Massachusetts Institute of Technology
Francis Bitter National Magnet Lab.
Cambridge, MA 02139

Dr. Gregory Canavan
Director, Office of Inertial Fusion
U. S. Department of Energy
M.S. C404
Washington, D.C. 20545

Prof. C. D. Cantrell
Center for Quantum Electronics
& Applications
The University of Texas at Dallas
P. O. Box 688
Richardson, TX 75080

Dr. Maria Caponi
TRW, Building R-1, Room 1070
One Space Park
Redondo Beach, CA 90278

Dr. J. Cary
Los Alamos National Scientific
Laboratory
MS 608
Los Alamos, NM 87545

Dr. Weng Chow
Optical Sciences Center
University of Arizona
Tucson, AZ 85721

Dr. Peter Clark
TRW, Building R-1, Room 1096
One Space Park
Redondo Beach, CA 90278

Dr. Robert Clark
P. O. Box 1925
Washington, D.C. 20013

Dr. William Colson
Quantum Institute
Univ. of California at Santa Barbara
Santa Barbara, CA 93106

Dr. William Condell
Code 421
Office of Naval Research
Arlington, VA 22217

Dr. Richard Cooper
Los Alamos National Scientific
Laboratory
P. O. Box 1663
Los Alamos, NM 87545

Cmdr. Robert Cronin
NFOIO Detachment, Suitland
4301 Suitland Road
Washington, D.C. 20390

Dr. R. Davidson (5 copies)
Plasma Fusion Center
Massachusetts Institute of
Technology
Cambridge, MA 02139

Dr. John Dawson (2 copies)
Physics Department
University of California
Los Angeles, CA 90024

Dr. David Deacon
Physics Department
Stanford University
Stanford, CA 94305

Defense Technical Information
Center (2 copies)
Cameron Station
5010 Duke Street
Alexandria, VA 22313

Dr. Francesco De Martini
Instituto de Fiscia
G. Marconi" Univ.
Piazzo delle Science, 5
ROMA00185 ITALY

Prof. P. Diament
Columbia University
Dept. of Electrical Engineering
New York, NY 10027

Prof. J. J. Doucet (5 copies)
Ecole Polytechnique
91128 Palaiseau
Paris, France

Dr. John Elgin (2 copies)
Imperial College
Dept. of Physics (Optics)
London SWF, England

Dr. Luis R. Elias (2 copies)
Quantum Institute
University of California
Santa Barbara, CA 93106

Dr. David D. Elliott
SRI International
33 Ravenswood Avenue
Menlo Park, CA 94025

Dr. Jim Elliot (2 copies)
X-Division, M.S. 531
Los Alamos National Scientific
Laboratory
Los Alamos, NM 87545

Director (2 copies)
National Security Agency
Fort Meade, MD 20755
ATTN: Mr. Richard Foss, A42

Dr. Robert Fossum, Director
(2 copies)
DARPA
1400 Wilson Boulevard
Arlington, VA 22209

Dr. Edward A. Frieman
Director, Office of Energy Research
U. S. Department of Energy
M.S. 6E084
Washington, D.C. 20585

Dr. George Gamota (3 copies)
OUSDRE (R&AT)
Room 3D1067, The Pentagon
Washington, D.C. 20301

Dr. Richard L. Garwin
IBM, T. J. Watson Research Center
P. O. Box 218
Yorktown Heights, NY 10598

Dr. Edward T. Gerry, President
W. J. Schafer Associates, Inc.
1901 N. Fort Myer Drive
Arlington, VA 22209

Dr. Avraham Gover
Tel Aviv University
Fac. of Engineering
Tel Aviv, ISRAEL

Mr. Donald L. Haas, Director
DARPA/STO
1400 Wilson Boulevard
Arlington, VA 22209

Dr. P. Hammerling
La Jolla Institute
P. O. Box 1434
La Jolla, CA 92038

Director
National Security Agency
Fort Meade, MD 20755
ATTN: Mr. Thomas Handel, A243

Dr. William Happer
560 Riverside Drive
New York City, NY 10027

Dr. Robert J. Hermann
Assistant Secretary of the
Air Force (RD&L)
Room 4E856, The Pentagon
Washington, D.C. 20330

Dr. Rod Hiddleston
KMS Fusion
Ann Arbor, MI 48106

Dr. J. L. Hirshfield (2 copies)
Yale University
Mason Laboratory
400 Temple Street
New Haven, CT 06520

Dr. R. Hofland
Aerospace Corp.
P. O. Box 92957
Los Angeles, CA 90009

Dr. Fred Hopf
University of Arizona
Tucson, AZ 85721

Dr. Benjamin Huberman
Associate Director, OSTP
Room 476, Old Executive Office Bldg.
Washington, D.C. 20506

Dr. S. F. Jacobs
Optical Sciences Center
University of Arizona
Tucson, AZ 85721

Dr. S. Johnston
216 Mudd Bldg.
Columbia University
New York, N.Y. 10027

Mr. Eugene Kopf
Principal Deputy Assistant
Secretary of the Air Force (RD&L)
Room 4E964, The Pentagon
Washington, D.C. 20330

Prof. N. M Kroll
La Jolla Institute
P. O. Box 1434
La Jolla, CA 92038

Dr. Tom Kuper
Optical Sciences Center
University of Arizona
Tucson, AZ 85721

Dr. Thomas Kwan
Los Alamos National Scientific
Laboratory
MS608
Los Alamos, NM 87545

Dr. Willis Lamb
Optical Sciences Center
University of Arizona
Tucson, AZ 85721

Mr. Mike Lavan
BMDATC-O
ATTN: ATC-O
P. O. Box 1500
Huntsville, AL 35807

Dr. John D. Lawson (2 copies)
Rutherford High Energy Lab.
Chilton
Didcot, Oxon OX11 OOX
ENGLAND

Mr. Ray Leadabrand
SRI International
333 Ravenswood Avenue
Menlo Park, CA 94025

Mr. Barry Leven
NISC/Code 20
4301 Suitland Road
Washington, D.C. 20390

Dr. Donald M. LeVine (3 copies)
SRI International
1611 N. Kent Street
Arlington, VA 22209

Dr. Anthony T. Lin
University of California
Los Angeles, CA 90024

Dr. A. Luccio - 725B
Brookhaven National Laboratories
Associated University, Inc.,
Upton, L.I., N.Y. 11973

Director (2 copies)
National Security Agency
Fort Meade, MD 20755
ATTN: Mr. Robert Madden, R/SA

Dr. John Madey
Physics Department
Stanford University
Stanford, CA 94305

Dr. Joseph Mangano
DARPA
1400 Wilson Boulevard
Arlington, VA 22209

Dr. S. A. Mani
W. J. Schafer Associates, Inc.
10 Lakeside Office Park
Wakefield, MA 01880

Dr. Mike Mann
Hughes Aircraft Co.
Laser Systems Division
Culver City, CA 90230

Dr. T. C. Marshall
Applied Physics Department
Columbia University
New York, NY 10027

Mr. John Meson
DARPA
1400 Wilson Boulevard
Arlington, VA 22209

Dr. Pierre Meystre
Projektgruppe fur Laserforschung
Max Planck Gesellschaft
Garching, MUNICH WEST GERMANY

Dr. Gerald T. Moore
Optical Sciences Center
University of Arizona
Tucson, Az 85721

Dr. Philip Morton
Stanford Linear Accelerator Center
P. O. Box 4349
Stanford, CA 94305

Dr. Jesper Munch
TRW
One Space Park
Redondo Beach, CA 90278

Dr. George Neil
TRW
One Space Park
Redondo Beach, CA 90278

Dr. Kelvin Neil
Lawrence Livermore National Lab.
Code L-321, P. O. Box 808
Livermore, CA 94550

Dr. Brian Newnam
MS 564
Los Alamos National Scientific Laboratory
P. O. Box 1663
Los Alamos, NM 87545

Dr. Milton L. Noble (2 copies)
General Electric Company
G. E. Electric Park
Syracuse, NY 13201

Prof. E. Ott (2 copies)
University of Maryland
Dept. of Physics
College Park, MD 20742

Dr. Richard H. Pantell
Stanford University
Stanford, CA 94305

Dr. Claudio Parazzoli
Highes Aircraft Company
Building 6, MS/C-129
Centinela & Teale Streets
Culver City, CA 90230

Dr. Richard M. Patrick
AVCO Everett Research Lab., Inc.
2385 Revere Beach Parkway
Everett, MA 02149

Dr. Claudio Pellegrini
Brookhaven National Laboratory
Associated Universities, Inc.
Upton, L.I., NY 11973

The Honorable William Perry
Under Secretary of Defense (R&E)
Office of the Secretary of Defense
Room 3E1006, The Pentagon
Washington, D.C. 20301

Dr. Alan Pike
DARPA/STO
1400 Wilson Boulevard
Arlington, VA 22209

Dr. Hersch Pilloff
Code 421
Office of Naval Research
Arlington, VA 22217

Dr. Charles Planner
Rutherford High Energy Lab.
Chiltón
Didcot, Oxon, OX11, OOX
ENGLAND

Dr. Michal Poole
Daresbury Nuclear Physics Lab.
Daresbury, Warrington
Cheshire WA4 4AD
ENGLAND

Dr. Don Prosnitz
Lawrence Livermore National Lab.
Livermore, CA 94550

Dr. D. A. Reilly
AVCO Everett Research Lab.
Everett, MA 02149

Dr. James P. Reilly
W. J. Schafer Associates, Inc.
10 Lakeside Office Park
Wakefield, MA 01880

Dr. A. Renieri
C.N.E.N.
Div. Nuove Attivita
Dentro di Frascatti
Frascatti, Rome
ITALY

Dr. Daniel N. Rogovin
SAI
P. O. Box 2351
La Jolla, CA 92038

Dr. Michael Rosenbluh
MIT - Magnet Laboratory
Cambridge, MA 02139

Dr. Marshall N. Rosenbluth
Institute for Advanced Study
Princeton, NJ 08540

Dr. Eugene Ruane (2 copies)
P. O. Box 1925
Washington, D.C. 20013

Dr. Antonio Sanchez
MIT/Lincoln Laboratory
Room B231
P. O. Box 73
Lexington, MA 02173

Dr. Aleksandr N. Sandalov
Department of Physics
Moscow University
MGU, Lenin Hills
Moscow, 117234, USSR

Prof. S. P. Schlesinger
Columbia University
Dept. of Electrical Engineering
New York, NY 10027

Dr. Howard Schlossberg
AFOSR
Bolling AFB
Washington, D.C. 20332

Dr. Stanley Schneider
Rotodyne Corporation
26628 Fond Du Lac Road
Palos Verdes Peninsula, CA 90274

Dr. Marlan O. Scully
Optical Science Center
University of Arizona
Tucson, AZ 85721

Dr. Steven Segel
KMS Fusion
3621 S. State Street
P. O. Box 1567
Ann Arbor, MI 48106

Dr. Robert Sepucha
DARPA/STO
1400 Wilson Boulevard
Arlington, VA 22209

Dr. A. M. Sessler
Lawrence Berkeley Laboratory
University of California
1 Cyclotron Road
Berkeley, CA 94720

Dr. Earl D. Shaw
Bell Labs
600 Mountain Avenue
Murray Hill, NJ 07974

Dr. Chan-Chin Shih
TRW, R1-1070
1 Space Park
Redondo Beach, CA 90278

Dr. Jack Slater
Mathematical Sciences, NW
P. O. Box 1887
Bellevue, WA 98009

Dr. Kenneth Smith
Physical Dynamics, Inc.
P. O. Box 556
La Jolla, CA 92038

Mr. Todd Smith
Hansen Labs
Stanford University
Stanford, CA 94305

Dr. Joel A. Snow
Senior Technical Advisor
Office of Energy Research
U. S. Department of Energy, M.S. E084
Washington, D.C. 20585

Dr. Richard Spitzer
Stanford Linear Accelerator Center
P. O. Box 4347
Stanford, CA 94305

Mrs. Alma Spring
DARPA/Administration
1400 Wilson Boulevard
Arlington, VA 22209

DRI/MP Reports Area G037 (2 copies)
333 Ravenswood Avenue
Menlo Park, CA 94025
ATTN: D. Leitner

Dr. Abraham Szoke
Lawrence Livermore National Lab.
MS/L-470, P. O. Box 808
Livermore, CA 94550

Dr. Milan Tekula
AVCO Everett Research Lab.
2385 Revere Beach Parkway
Everett, MA 02149

Dr. John E. Walsh
Department of Physics
Dartmouth College
Hanover, NH 03755

Dr. Wasneski (2 copies)
Naval Air Systems Command
Department of the Navy
Washington, D.C. 20350

Ms. Bettie Wilcox
Lawrence Livermore National Lab.
ATTN: Tech. Info. Dept. L-3
P. O. Box 808
Livermore, CA 94550

Dr. A. Yariv
California Institute of Tech.
Pasadena, CA 91125